

1 Title

2 Insights into the origin of metazoan multicellularity from predatory unicellular relatives of
3 animals

4 Authors

5 Denis V. Tikhonenkov^{1,2*}, Elisabeth Hehenberger³, Anton S. Esaulov⁴, Olga I. Belyakova⁴, Yuri
6 A. Mazei⁵, Alexander P. Mylnikov^{1,†}, Patrick J. Keeling²

7 Affiliations

8 ¹Papanin Institute for Biology of Inland Waters, Russian Academy of Sciences, Borok, 152742,
9 Russia

10 ²Department of Botany, University of British Columbia, Vancouver, V6T 1Z4, British
11 Columbia, Canada.

12 ³GEOMAR - Helmholtz Centre for Ocean Research Kiel, Division of Experimental Ecology,
13 Duesternbrookerweg 20, 24105 Kiel, Germany

14 ⁴Penza State University, Penza, 440026, Russia

15 ⁵Moscow State University, Moscow, 119991, Russia

16 †Deceased 30 May 2019

17 *Correspondence to: tikho-denis@yandex.ru, pkeeling@mail.ubc.ca

18

19 Abstract

20 The diversity and biology of unicellular relatives of animals has strongly informed our
21 understanding of the transition from single-celled organisms to the multicellular Metazoa. Here
22 we analyse the cellular structures and complex life cycles of the novel unicellular holozoans
23 *Pigoraptor* and *Syssomonas* (Opisthokonta). Both lineages are characterized by complex life
24 cycles with a variety of cell types, the formation of multicellular aggregations and syncytium-
25 like structures, and an unusual diet for single-celled opisthokonts (partial cell fusion and joint
26 sucking of a large eukaryotic prey), all of which provide new insights into the origin of
27 multicellularity in Metazoa. The ability to feed on large eukaryotic prey could have been a
28 powerful trigger in the formation and development both aggregative (e.g., joint feeding, which
29 also implies signalling) and clonal (e.g., hypertrophic growth followed by palintomy)
30 multicellular stages that played important roles in the emergence of multicellular animals.

31

32 Introduction

33 The origin of animals (Metazoa) from their unicellular ancestors is one of the most
34 important evolutionary transitions in the history of life. Questions about the mechanisms of this

35 transformation arose about 200 years ago, but is still far from being resolved today. Most
36 investigations on the origin of Metazoa have focused on determining the nature of the shared,
37 multicellular ancestor of all contemporary animals (Moroz et al., 2014; Srivastava et al., 2008;
38 2010). However, even the branching order of early, non-bilaterian lineages of animals on
39 phylogenetic trees is still debated: some consider either sponges (Porifera) (Feuda et al., 2017;
40 Philippe et al., 2009; Simion et al., 2017;) or Ctenophora (Dunn et al., 2008; Ryan et al., 2013;
41 Whelan et al., 2015) or Placozoa (Schierwater et al., 2009; Signorovitch et al., 2007;) to be the
42 first branch of extant metazoans. While molecular clock-based studies and paleontological
43 evidence indicate that multicellular animals arose more than 600 million years ago (Maloof et
44 al., 2010; Sharpe et al., 2015), we know less about how animals arose. To establish the sequence
45 of events in the origin of animals from unicellular ancestors, we also need to investigate their
46 closest relatives, the unicellular opisthokont protists. Information on the diversity and biology of
47 the unicellular relatives of animals, their placement within the phylogenetic tree of opisthokonts,
48 and the identification of molecular and morphological traits thought to be specific for animals
49 within their unicellular sisters, have all strongly informed our understanding of the transition
50 from single-celled organisms to the multicellular Metazoa (King et al., 2008; Suga et al., 2013;
51 Suga, Ruiz-Trillo, 2013; Torruella et al., 2015).

52 Until recently, only three unicellular lineages, the choanoflagellates, filastereans,
53 ichthyosporeans, as well as *Corallochytrium limacisporum*, a mysterious marine osmotrophic
54 protist described in association with corals, have been described as collectively being sisters to
55 animals. Together with animals they form the Holozoa within the Opisthokonta (Aleshin et al.,
56 2007; Lang et al., 2002; Torruella et al., 2015). These unicellular organisms have extremely
57 variable morphology and biology. Choanoflagellates represent a species-rich group of filter-
58 feeding, bacterivorous, colony-forming protists, which possess a single flagellum surrounded by
59 a collar of tentacles (microvilli). They are subdivided into two main groups – the predominantly
60 marine Acanthoecida and the freshwater and marine Craspedida (Carr et al., 2017). Filastereans
61 are amoeboid protists producing pseudopodia. Until recently, they were represented by only two
62 species: the endosymbiont of a freshwater snail, *Capsaspora owczarzaki*, and the free-living
63 marine heterotroph, *Ministeria vibrans* (Hertel et al., 2002; Shalchian-Tabrizi et al., 2008),
64 which was recently shown to also possess a single, real flagellum (Mylnikov et al., 2019).
65 Ichthyosporeans are parasites or endocommensals of vertebrates and invertebrates characterized
66 by a complex life cycle, reproduction through multinucleated coenocytes colonies and flagellated
67 and amoeboid dispersal stages (Suga, Ruiz-Trillo, 2013). *Corallochytrium* is a unicellular
68 coccoid organism, which produces rough, raised colonies and amoeboid limax-like spores

69 (Raghukumar, 1987.). Additionally, molecular data predict a cryptic flagellated stage for
70 *Corallochytrium* (Torruella et al., 2015).

71 A large number of hypotheses about the origin of multicellular animals have been
72 proposed. The most developed model for the origin of metazoan multicellularity is based on a
73 common ancestor with choanoflagellates (James-Clark, 1866; Ivanov, 1967; King et al., 2008,
74 Mikhailov et al., 2009; Nielsen, 1987, Ratcliff et al., 2012). This idea was initially based on the
75 observed similarity between choanoflagellates and specialized choanocyte cells in sponges.
76 Molecular investigations also supported the idea by consistently indicating that choanoflagellates
77 are the closest sister group to Metazoa. However, molecular phylogeny itself does not reveal the
78 nature of ancestral states, it only provides a scaffolding on which they might be inferred from
79 other data. The evolutionary positions of the other unicellular holozoans (filastereans,
80 ichthyosporeans, and *Corallochytrium*) are less clear and sometimes controversial (e.g. Cavalier-
81 Smith, Chao, 2003; del Campo, Ruiz-Trillo, 2013; Hehenberger et al., 2017; Medina et al., 2003;
82 Ruiz-Trillo et al., 2008; Shalchian-Tabrizi et al., 2008; Torruella et al., 2012, 2015;).

83 As noted above, many molecular traits that were thought to be “animal-specific” are now
84 known to be present in unicellular holozoans, while conversely the loss of other traits have been
85 shown to correlate with the origin of the animals. But gene content alone is not sufficient to
86 provide a comprehensive understanding of the cell biology, life cycle and regulation capabilities
87 of the unicellular ancestor, it requires also analysis of the biology of the extant unicellular
88 relatives of animals (Sebé-Pedrós et al., 2017).

89 Recently we described a phylogenomic and transcriptome analyses of three novel
90 unicellular holozoans (Hehenberger et al., 2017), which are very similar in morphology and life
91 style but not closely related. *Pigoraptor vietnamica* and *Pigoraptor chileana* are distantly related
92 to filastereans, and *Syssomonas multiformis* forms a new phylogenetic clade, “Pluriformea”, with
93 *Corallochytrium*. Both new genera of unicellular holozoans form the shortest and most slowly
94 evolving branches on the tree, which improved support for many nodes in the phylogeny of
95 unicellular holozoans. Also, comparison of gene content of the new taxa with the known
96 unicellular holozoans revealed several new and interesting distribution patterns for genes related
97 to multicellularity and adhesion (Hehenberger et al., 2017).

98 Here we report the detailed morphological and ultrastructural analyses of these new
99 species, as well as describing their life cycle in culture, which are important implications for
100 understanding the origin of animals as are the genetic analyses. All three species are shown to be
101 predatory flagellates that feed on large eukaryotic prey, which is very unusual for unicellular
102 Holozoa. They also appear to exhibit complex life histories with several distinct stages,
103 including interesting multicellular structures that might offer important clues as to precursors of

104 multicellularity. On the basis of these findings we discuss the current hypotheses about the origin
105 of multicellular animals from their unicellular ancestors.

106

107 **Results and discussion**

108

109 Detailed morphological descriptions of the cells and their aggregates are presented below.

110

111 *Syssomonas multiformis* Tikhonenkov, Hehenberger, Mylnikov et Keeling 2017

112

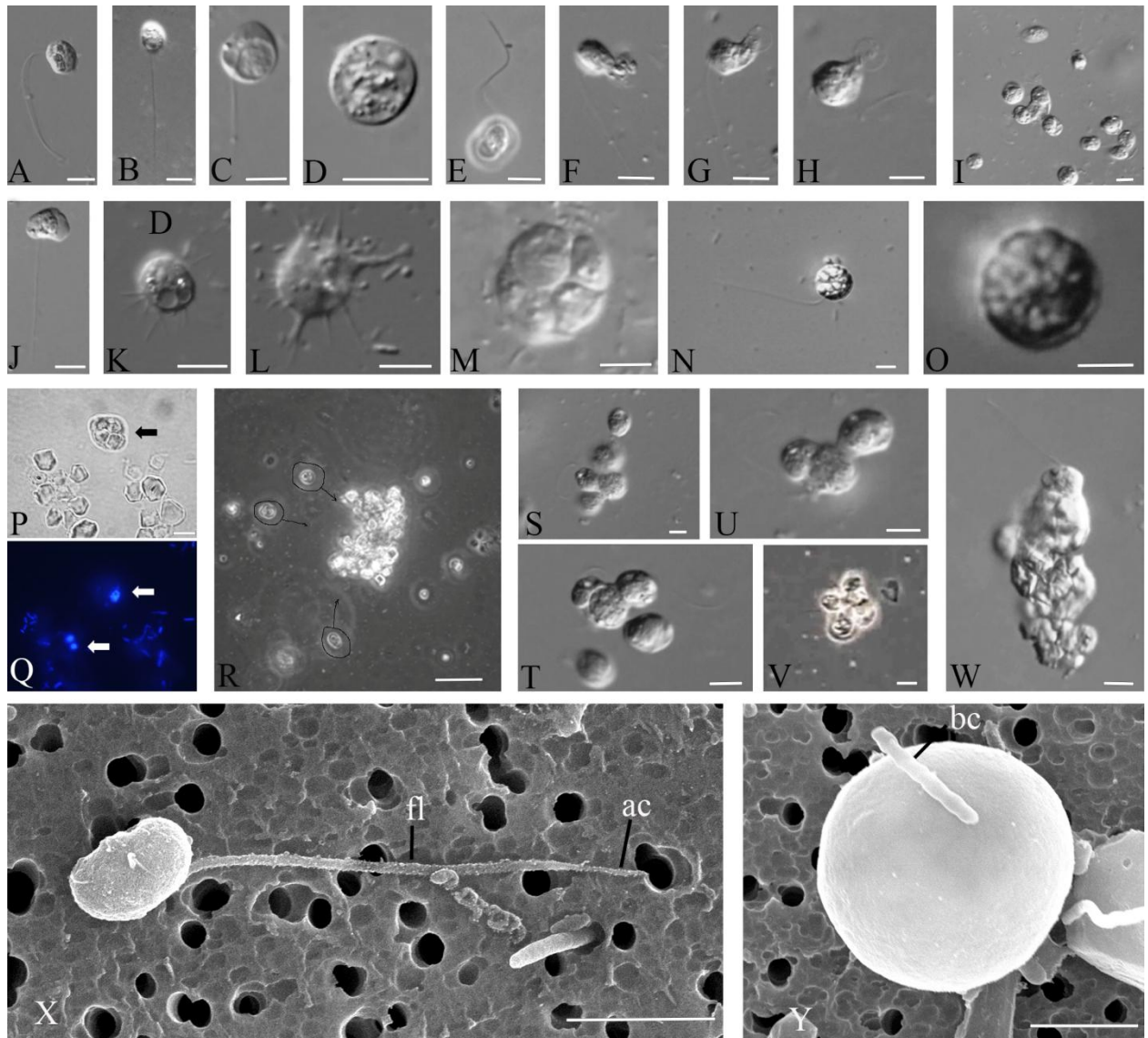
113 **Morphology and life cycle**

114 The organism is characterized by a large variety of life forms including flagellates,
115 amoebflagellates, amoeboid non-flagellar cells, and spherical cysts. The most common stage in
116 the life cycle, a swimming flagellate cell, resembles a typical opisthokont cell, reminiscent of
117 sperm cells of most animals and zoospores of the chytrid fungi. Cells are round-to-oval and
118 propel themselves with a single, long posterior flagellum (Fig. 1A-C, X). The flagellum is
119 smooth and emerges from the middle-lateral point of the cell, turns back and always directs
120 backward during swimming. The cell rotates during swimming (Video 1). Flagellar beating can
121 be very fast, which can create the appearance of two flagella. Motile flagellates can suddenly
122 stop and change the direction of movement. The flagellated cells measure 7-14 μm in diameter.
123 The flagellum length is 10-24, rarely 35 μm . Cyst diameter is 5 μm (Fig. 1D, Y).

124 Solitary cells of *Syssomonas* can temporarily attach to the substrate by the anterior part of
125 the cell body. They produce water flow by rapid flagellum beating posteriorly and in that state
126 resemble cells of choanoflagellates or choanocytes from sponges (Fig. 1E, Video 2). Floating
127 flagellated cells can also move to the bottom and transform to amoebflagellates (Fig. 1J, Video
128 3) by producing both wide lobopodia and thin short filopodia. Flagellar beating becomes slower
129 and then stops. Amoebflagellates crawl along the surface using their anterior lobopodia and can
130 take up clusters of bacteria. The organism can lose the flagellum via three different modes: the
131 flagellum may be abruptly discarded from its proximal part of the cell; a stretched flagellum may
132 be retracted into the cell; the flagellum may convolve under the cell-body and then retract into
133 the cell as a spiral (Video 4). As a result *Syssomonas* turns into an amoeba (Fig. 1K,L, Video 4).
134 Amoeboid cells produce thin, relatively short filopodia and sometimes have two contractile
135 vacuoles. Amoeboid cells are weakly motile. The transformation of amoebflagellates and
136 amoebae back to flagellates was also observed.

137 Amoeboid cells can also retract their filopodia, become roundish and transform into a cyst
138 (Fig. 1D, Video 5). Palintomic divisions may occur inside the cyst and up to 16 (2, 4, 8, or 16)

139 flagellated cells are released as a result (Fig. 1M, Video 6). Division into two cell structures was
140 also observed in culture (Video 7), but it is hard to tell whether a simple binary longitudinal
141 division of a *Syssomonas* cell with retracted flagellum has taken place, or the final stage of a
142 division inside the cyst has been observed.



143

144 Fig.1. External morphology and life forms of *Syssomonas multififormis*. A-C – swimming
145 flagellated cells; D – cyst; E – attached flagellated cell; F-H – sucking of eukaryotic prey; I –
146 simultaneous joint feeding of three cells of *Syssomonas* on one prey cell with attraction of other
147 specimen to the feeding spot; J – amoeboflagellate; K,L – amoeboid cell; M – palintomic cell-
148 division inside the cyst; N – cell with inside vesicles; O – cyst with vesicles; P,Q – cells of
149 *Syssomonas* engulfed starch granules (bright field (P) and fluorescent microscopy, DAPI
150 staining); R – cells of *Syssomonas* with engulfed starch granules hiding into the starch druse, S-
151 U, W – cell aggregations of *Syssomonas* near the bottom of Petri dish; V – floating aggregation
152 of flagellated cells; X – general view of flagellated cell (SEM), Y – cyst (SEM). Scale bars: A-P,
153 S-W – 10 μ m, R – 100 μ m, X – 3 μ m, Y – 2 μ m.

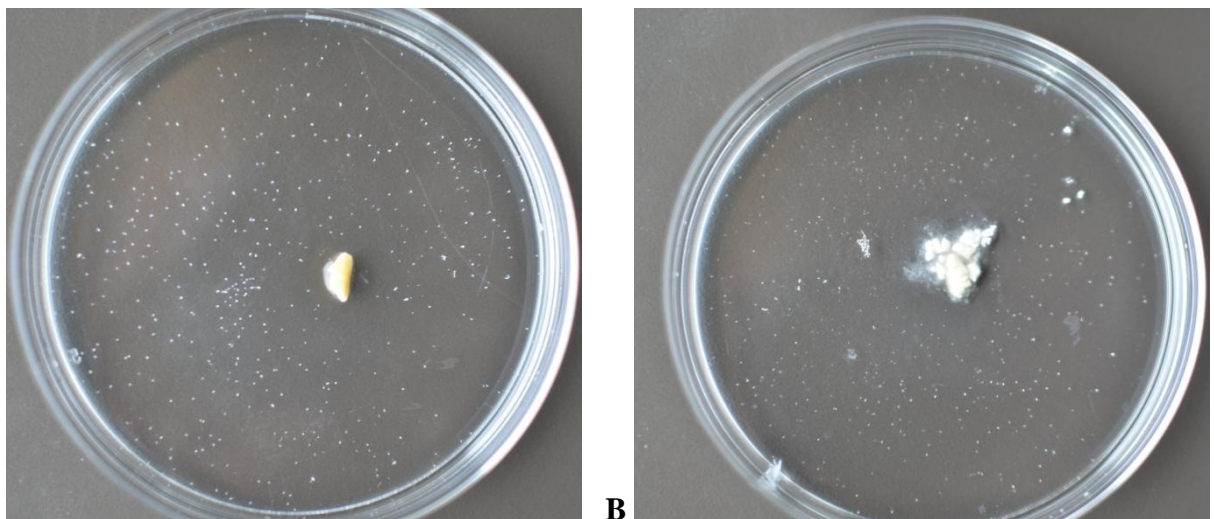
154

155 Floating, flagellated cells containing vesicular structures were observed (Fig. 1N, Video 8),
156 however the process of formation and the purpose of these vesicles is unknown. After some time

157 such cells lose their flagellum and transform into vesicular cysts with a thick cover (Fig. 1O).
158 Division inside vesicular cysts was not observed within 10 days of observation. Such structures
159 could represent resting cysts or dying cells containing autophagic vacuoles (the partial
160 destruction of one such cyst was observed after 4 days of observation, see Video 8).

161 The organism is a predator; it takes up other flagellates (e.g. *Parabodo caudatus* and
162 *Spumella* sp.) which can be smaller, about the same size, or larger than *Syssomonas*. But in
163 contrast to many other eukaryotrophic protists, *Syssomonas* does not possess any extrusive
164 organelles for prey hunting. After initial contact, *Syssomonas* attaches to the prey cell and sucks
165 out their cytoplasm (without ingesting the cell membrane) (Fig. 1F-H, Video 9). The organism
166 feeds better on inactive, slow moving or dead cells and can also capture intact prey cells and
167 cysts by means unobserved. After attaching to the prey, many other *Syssomonas* cells become
168 attracted to the same prey cell (likely by chemical signaling) and try to attach to it. Joint feeding
169 was observed: several cells of *Syssomonas* can suck out the cytoplasm of the same prey cell
170 together (Fig. 1I, Video 9).

171 In culture, *Syssomonas* can take up starch granules from rice grains, the granules can be the
172 same size as the cells (Fig. 1P,Q). In the presence of *Syssomonas* cells, rice grains in Petri dishes
173 crumble into small fragments and separate granules of starch (Fig. S1). Cells of *Syssomonas* with
174 engulfed starch granules can hide within the starch druses and lose the flagellum (Fig. 1R).
175 Numerous cysts integrated into the starch matrix were often observed in culture.



176 **A**
177 Fig. S1. Rice grain destruction in Petri dish with Pratt medium and presence of the cells of
178 *Parabodo caudatus* (prey) only (A) and *Syssomonas multififormis* (B) after 9 days of
179 incubation.
180

181 The organism can also feed on clusters of bacteria (Video 10) using short pseudopodia.
182 After feeding, *Syssomonas* cells become 2-3 times bigger and a large food vacuole is formed at
183 the posterior end of the cell-body (Fig. 1C). In the absence of eukaryotic prey (cultivation on

184 bacteria and/or rice grain/starch only), *Syssomonas* either dies or forms resting cysts. Bacteria
185 alone are not sufficient food for *Syssomonas*.

186 Solitary cells of *Syssomonas* can partially merge and form temporary cell aggregations.
187 They are usually shapeless, observed near the bottom, and consist of about 3-10 flagellated or
188 non-flagellated cells (Fig. 1S-U, Video 11). Another type of aggregation is formed by only
189 flagellated cells with outwards-directed flagella that can float in the water column and resemble
190 the rosette-like colonies of choanoflagellates (Fig. 1V, Video 12). Both types of aggregations
191 break up easily and it seems that the membranes of such aggregated cells are not fused.

192 However, in rich culture, solitary cells of *Syssomonas* can sometimes merge completely at
193 the bottom of the Petri dish and form syncytium-like (or pseudoplasmodium) structures (it seems
194 that nuclei do not merge after cell fusion). The budding of young flagellated daughter cells from
195 such syncytia was observed (Video 13). Such syncytial structures with budding daughter cells
196 have not been observed in other eukaryotes, to our knowledge, but multinucleated structures
197 arising as a result of multiple cell aggregations or fusions of uninuclear cells are also known in
198 Dictyostelia (Eumycetozoa) and *Copromyxa* (Tubulinea) in the Amoebozoa (sister group of
199 Opisthokonta), as well as in other protists, such as Acrasidae in the Excavata, *Sorogena* in the
200 Alveolata, *Sorodiplophrys* in the Stramenopiles, and *Guttulinopsis* in the Rhizaria (Brown et al.,
201 2012). Within the opisthokonts, aggregation of amoeboid cells is only known in the sorocarpic
202 species *Fonticula alba* (Holomycota) (Brown et al., 2009). We should also note that a syncytium
203 is not an unusual cell structure in many fungi and animals; e.g. most of the cytoplasm of glass
204 sponges (Hexactinellida), the teguments of flatworms as well as the skeletal muscles and the
205 placenta of mammals (Gobert et al., 2003; Leyset al., 2006) have a syncytial structure.

206 In *Syssomonas*, the processes of cells merging attracts (again, likely by chemical
207 signalling) many other cells of *Syssomonas*, which actively swim near aggregates or syncytium-
208 like structures and try to attach to them. Some of these cells succeed to merge and the
209 aggregates grow.

210 All aggregations and syncytial-like structures do not seem to form by cell division, but
211 rather by a merger of the population of cells in the culture (although all cells in the clonal culture
212 are offspring of a single cell of *Syssomonas*).

213 All of the above-described life forms and cellular changes do not represent well-defined
214 phases of the life cycle of *Syssomonas*, but rather embody temporary transitions of cells in
215 culture which are reversible.

216 *Syssomonas* grows at room temperature (22°C) and can survive at temperatures from +5 to
217 36 °C. At high temperature (30-35 °C) the prey cells (bodonids) in culture become immobile and
218 roundish; *Syssomonas* actively feeds on such easily accessible cells, multiplies and produces

219 high biomass. In the absence of live eukaryotic prey, increasing the incubation temperature does
220 not lead to an increase in cell numbers. The cells grow at pH values from 6 to 11. Agitation of
221 culture does not lead to the formation of cell aggregates as was observed in the filasterean
222 *Capsaspora* (Sebé-Pedrós et al., 2013b).

223

224 **Cell ultrastructure**

225 The cell is naked and surrounded by the plasmalemma. The naked flagellum ends in a
226 short, narrowed tip – the acroneme (Fig. 1X, 2D). A single spiral or other additional elements
227 (e.g. a central filament typical for choanoflagellates) in the transition zone of the flagellum were
228 not observed (Fig. 2B, 2C). The flagellar axoneme has an ordinary structure (9+2) in section (not
229 shown). The flagellum can be retracted into the cell (Fig. 2E). A cone-shaped rise at the cell
230 surface around the flagellum base was observed (Fig. 2B, 2C). The flagellar transition zone
231 contains a transversal plate which is located above the cell surface (Fig. 2B).

232 Two basal bodies, one flagellar and one non-flagellar (Fig. 2A–C), lie approximately at a
233 45-90 degrees angle to each other (Fig. 2B, 2C). The flagellar root system consists of several
234 elements. Arc-like dense material, representing satellites of the kinetosome, is connected with
235 the flagellar basal body and initiates microtubules which run into the cell (Fig. 2F). Radial fibrils
236 originate from the flagellar basal body (Fig. 3A-C, 3G) and resemble transitional fibres. At least
237 two fibrils connect to the basal bodies (Fig. 2B). It can be seen from serial sections that
238 microtubules originate near both basal bodies (Fig. 3 A–F). Dense (osmiophilic) spots are
239 situated near the basal bodies and some of them initiate bundles of microtubules (Fig. 3 I,J,L).
240 Microtubules originating from both basal bodies singly or in the form of a fan probably run into
241 the cell (Fig. 2 B, Fig. 3F–K). One group of contiguous microtubules begins from the dense spot
242 (Fig. 3L) and goes superficially close to the plasmalemma (Fig. 3 E,F,L).

243 The nucleus is 2.6 μm in diameter, has a central nucleolus and is situated closer to the
244 posterior part of the cell (Fig. 2 A, D, Fig. 4 H). The Golgi apparatus is of usual structure and is
245 positioned close to the nucleus (Fig. 2B, Fig. 4A). The cell contains several mitochondria with
246 lamellar cristae (Fig. 4 B–D). Unusual reticulate or tubular crystal-like structures of unknown
247 nature were observed inside the mitochondria (Fig. 4C, D). A contractile vacuole is situated at
248 the periphery of the cell and is usually surrounded by small vacuoles (Fig. 4E).

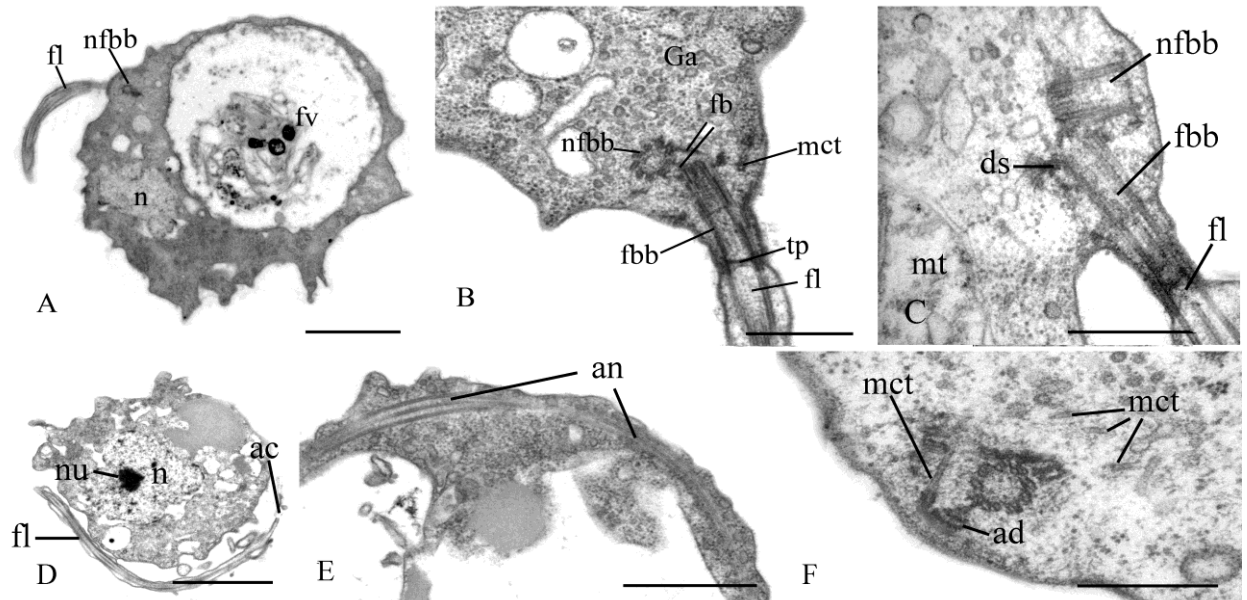
249 A large food vacuole is usually located posteriorly or close to the cell center and contains
250 either remnants of eukaryotic prey, e.g. cells (paraxial flagellar rods are seen) or cysts (fibrous
251 cyst envelope is seen) of *Parabodo caudatus*, or starch granules (Fig. 2A, Fig. 4F–H).
252 Exocytosis occurs on the posterior cell end (Fig. 4I).

253 Thin filopodia are located on some parts of cell surface (Figs. 4D, 4J).

254 Storage compounds are represented by roundish (presumably glycolipid) granules 0.8 μm
255 in diameter (Fig. 4 A,D,J).

256 A flagellum or flagellar axoneme, or two kinetosomes, as well as an eccentric nucleus,
257 mitochondria with lamellate cristae and dense matrix, and a food vacuole with remnants of the
258 prey cells are all visible inside cysts containing dense cytoplasm (Fig. 4K, L).

259 Extrusive organelles for prey hunting were not observed in any cell type.

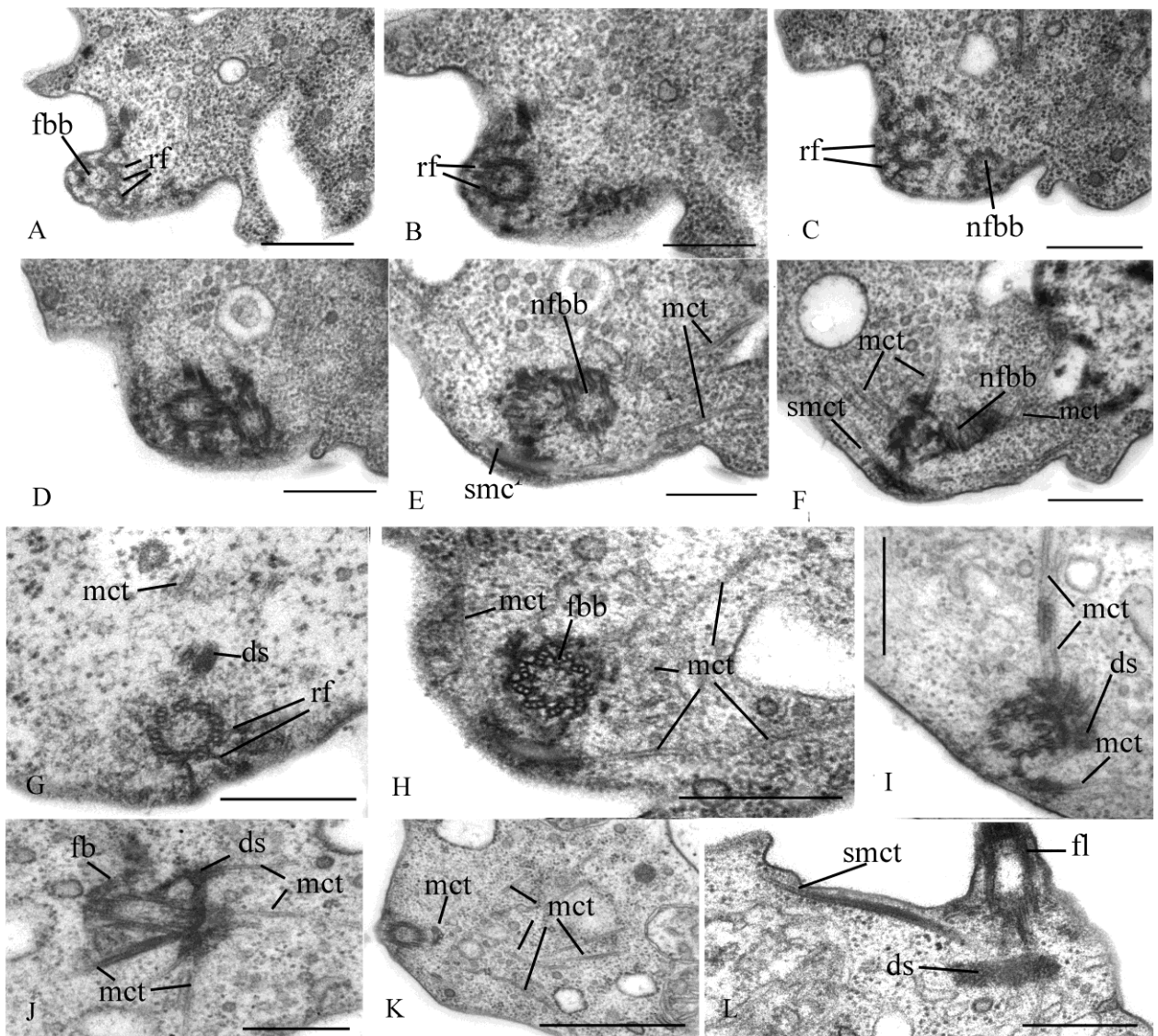


260
261 Fig. 2. General view and flagellum structure of *Syssomonas multiformis* (TEM). A –
262 general view of the cell section, B,C – arrangement of flagellum and basal bodies, D – twisting
263 of the flagellum around the cell, E – retracted flagellum axoneme inside the cell, F – basal body
264 of the flagellum and nearest structures.

265 ac – acroneme, ad – arc-like dense structure, an – flagellum axoneme, ds – dense spot, fb –
266 fibril, fbb – flagellar basal body, fl – flagellum, fv – food vacuole, Ga – Golgi apparatus, mct –
267 microtubule, mt – mitochondrion, n – nucleus, nfbb – non-flagellar basal body, nu – nucleolus,
268 tp – transversal plate.

269 Scale bars: A – 2, B – 0.5, C – 0.5, D – 2, E – J – 0.5 μm .

270

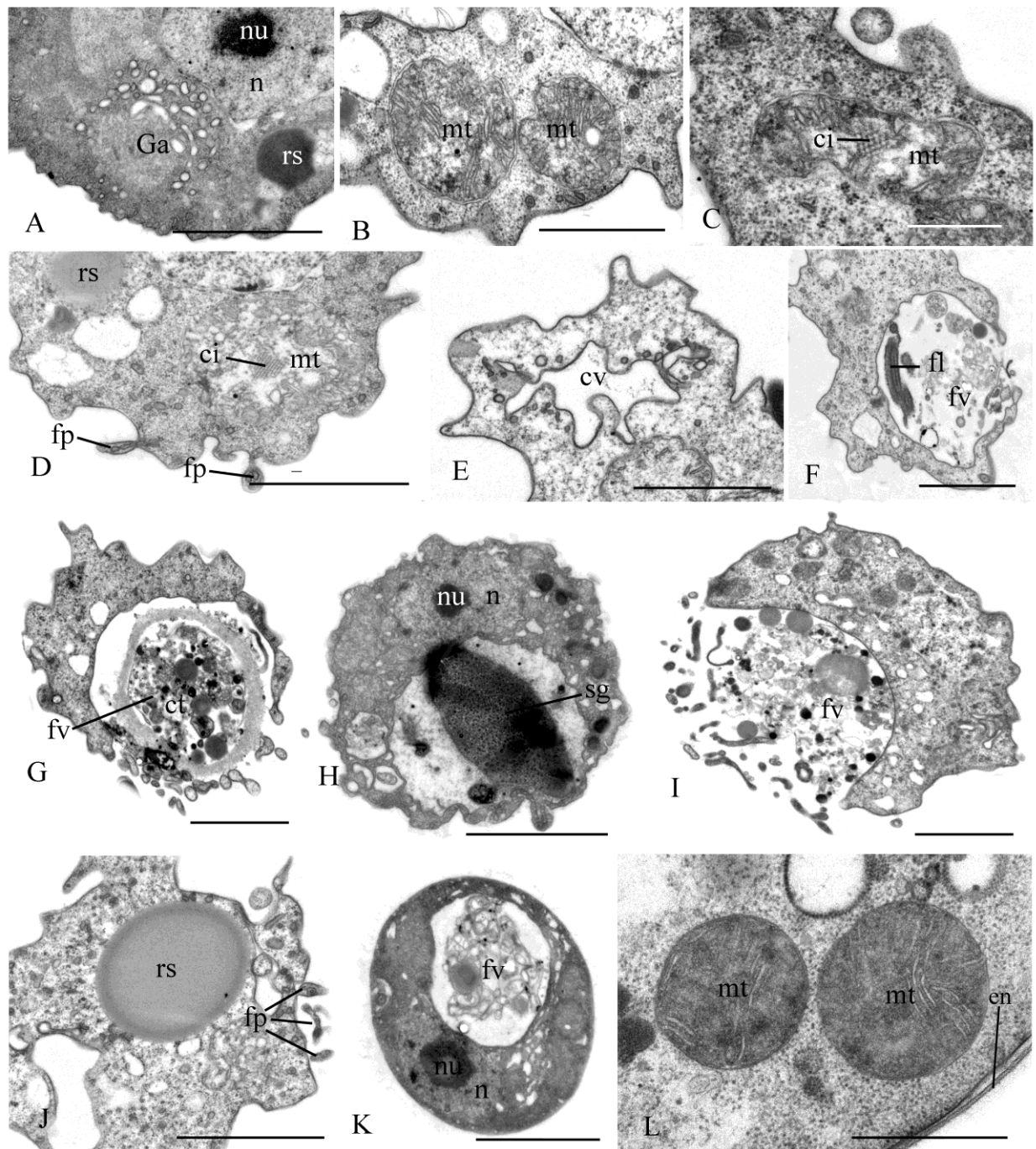


271
272
273
274
275
276
277

Fig. 3. Arrangement of kinetosomes of *Syssomonas multiformis*. A – F – serial sections of the kinetosomal area, G–L – structures nearby the kinetosomes.

ds – dense spot, fb – fibril, fbb – flagellar basal body, mct – microtubule, nfb – non-flagellar basal body, rf – radial fibrils, smct – submembrane microtubules.

Scale bars: A–J, L – 0.5, K – 1 μm.



278

279

280

281

282

283

284

285

286

287

288

289

290

291

Fig. 4. Cell structures and organelles of *Syssomonas multififormis*. A – Golgi apparatus, B –
 D – mitochondria, E – contractile vacuole, F – food vacuole with remnants of eukaryotic prey
 (*Parabodo*), flagella and paraxial rods are seen, G – food vacuole containing cyst of *Parabodo*,
 H – food vacuole containing starch granule, I – Exocytosis of food vacuole, J – reserve substance
 and filopodia, K – L – cysts.

ci – crystalloid inclusion, ct – cyst of the prey cell, cv – contractile vacuole, en – cyst
 envelope, fl – flagellum, fp – filopodia, fv – food vacuole, ga – Golgi apparatus, mt –
 mitochondrion, n – nucleus, nu – nucleolus, rs – reserve substance, sg – starch granule.

Scale bars: A – 2, B – 1, C – 0.5, D – 2, E – 2, F – 2, G – 2, H – 2, I – 2, J – 2, K – 2, L – 1
 µm.

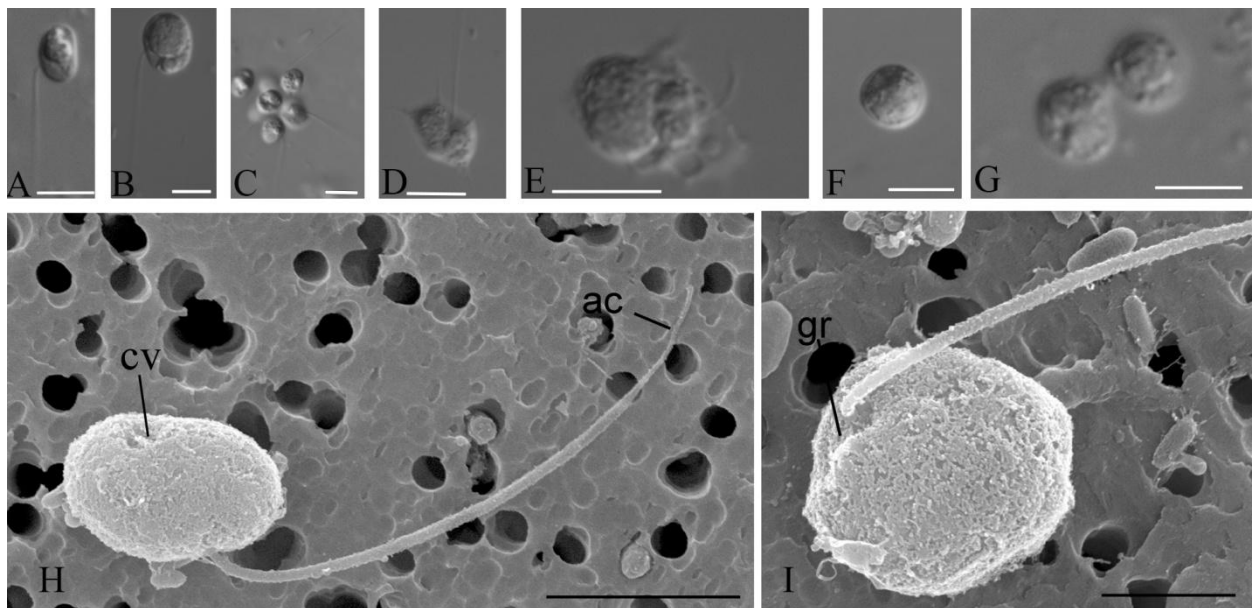
292 *Pigoraptor vietnamica* Tikhonenkov, Hehenberger, Mylnikov et Keeling 2017

293

294 **Morphology and life cycle**

295 The uniflagellated, elongated-oval cells are 5-12 μm long (Fig. 5 A,B,H,I). The flagellum
296 length is 9-14 μm . Saturated cells with a large food vacuole become roundish. The body plan,
297 movement, feeding, and growth conditions of *Pigoraptor* are identical to *Syssomonas*
298 *multiformis*, except for the feeding on starch granules, which was not observed in *Pigoraptor*.

299 The main stage of the life cycle is a swimming flagellated cell, which can form thin long,
300 sometimes branching filopodia that can attach to the substrate (Fig. 5D). Wide lobopodia were
301 also observed on some cells (Fig. 5E). Non-flagellate crawling amoebas were not observed.
302 *Pigoraptor* cells can retract the flagellum and become roundish. After several hours, such
303 spherical cells either divide into two daughter cells or turn into cysts (Fig. 5F), which stay intact
304 for a long period. Binary division was observed also inside the cyst (Fig. 5G), resulting in two
305 daughter cells that produce flagella and disperse.



306

307 Fig. 5. External morphology and life forms of *Pigoraptor vietnamica*. A, B, H, I – general
308 view of the cell (DIC and CEM); C – aggregation of flagellated cells; D – amoeboflagellate with
309 filopodia; E – cell with lobopodia; F – cyst; G – binary division.

310

ac – acroneme, cv – contractile vacuole, gr – groove.

311

Scale bars: A-G – 10; H – 4, I – 2 μm .

312

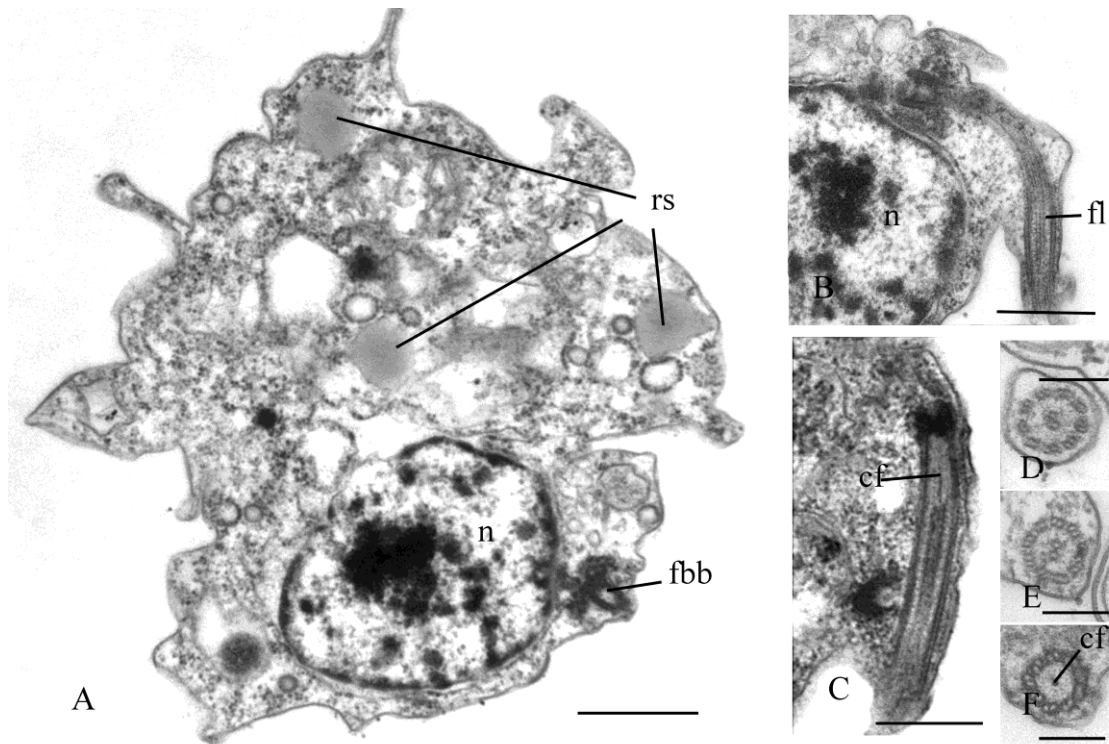
313 Cells of *Pigoraptor vietnamica* also form easily disintegrating aggregations (Fig. 5C) and
314 feed jointly (Video 14). The adjacent cells can partially merge during feeding. These
315 processes also seem to attract many other cells of *Pigoraptor*.

316

317 **Cell ultrastructure**

318 A single, naked flagellum with an acroneme originates from a small lateral groove and
319 directs backward (Fig. 5 H,I). The cell is naked and surrounded by the plasmalemma. Two basal
320 bodies, flagellar and non-flagellar, are located near the nucleus, lie approximately at a 90 degrees
321 angle to each other and are not connected by visible fibrils (Fig. 6 A,B; Fig. 7 A,B; Fig. 8 A–F).
322 The flagellum axoneme has an ordinary structure (9+2) in section (Fig. 6 D,E). A thin central
323 filament, which connects the central pair of microtubules to the transversal plate, was observed
324 (Fig. 6 C,F). The flagellum can be retracted into the cell (Fig. 9C). The flagellar root system is
325 reduced. Radial fibrils arise from the flagellar basal body (Fig. 7C). Microtubules pass near the
326 flagellar basal body (Fig. 7B, Fig. 8 E,F). Serial sections show that the non-flagellar basal body
327 does not initiate the formation of microtubules (Fig. 8 A,B)

328 The roundish nucleus is about 1.5 μm in diameter, contains a prominent nucleolus (Fig. 6
329 A,B, Fig. 7A, Fig. 9 A, D), and is situated closer to the posterior end of the cell. Chromatin
330 granules (clumps) are scattered within the nucleoplasm. The Golgi apparatus is adjacent to the
331 nucleus (Fig. 9B). Cells contain several mitochondria that possess lamellar cristae (Fig. 9 A,C).
332 Rare thin filopodia have been observed on the cell surface (Fig. 9 D,E). Cells usually contain one
333 large food vacuole (Fig. 9F), which contains remnants of eukaryotic prey and bacteria.
334 Exocytosis takes place on the anterior cell end (Fig. 9G). Storage compounds are represented by
335 roundish (presumably glycolipid) granules 0.3-0.4 μm in diameter (Fig. 6A, 7A, 9 C,H). Cells
336 contain symbiotic bacteria, which are able to divide in the host cytoplasm (Fig. 9 H,I). A single
337 contractile vacuole is situated close to the cell surface (not shown on cell sections but visualized
338 by TEM, Fig. 5H).

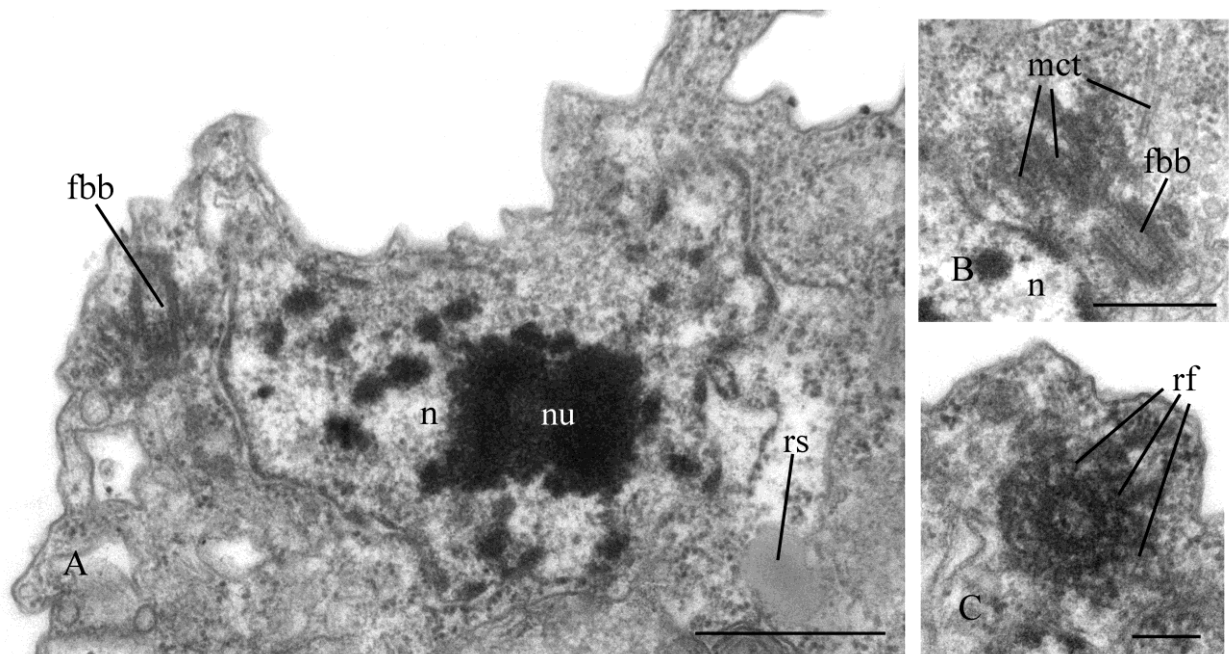


339
340
341
342
343
344
345
346

Fig. 6. General view and flagellum structure of *Pigoraptor vietnamica*, TEM. A – longitudinal cell section. B–C – longitudinal section of flagellum, D–F – transverse flagellum sections in transitional area.

cf – central filament, fbb – flagellar basal body, fl – flagellum, n – nucleus, rs – reserve substance.

Scale bars: A – 1, B – 0.5, C – 0.5, D – F – 0.2 – μm .



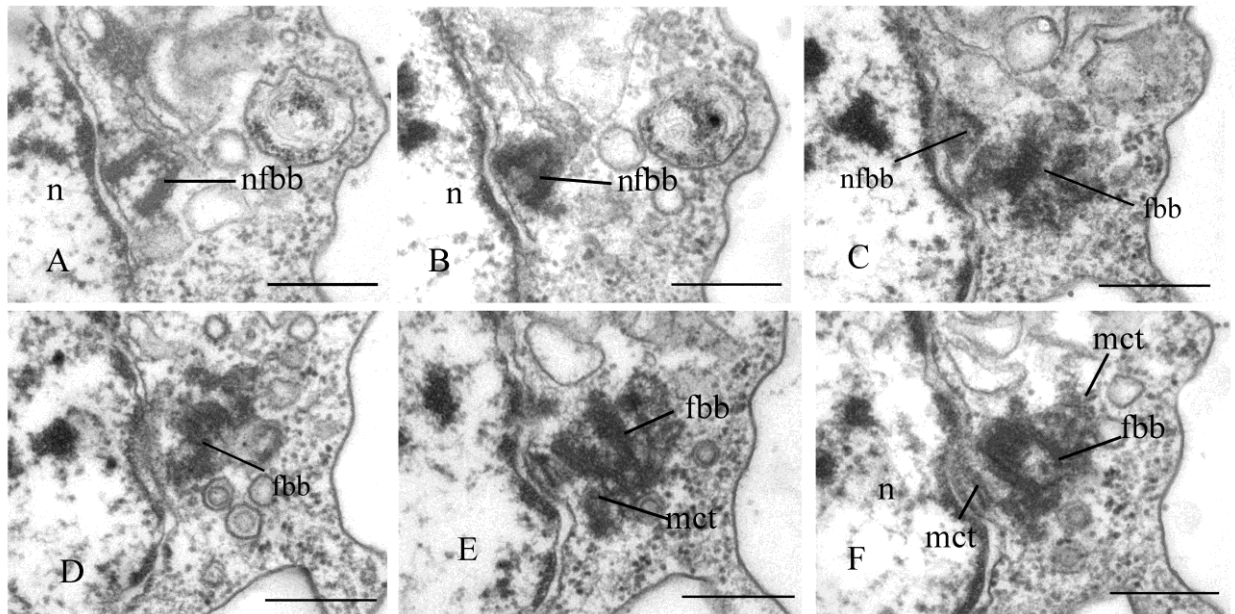
347
348
349
350
351
352
353
354

Fig. 7. Nucleus and arrangement of basal bodies of *Pigoraptor vietnamica*. A – part of the cell containing nucleus and flagellar basal body, B – non-flagellar basal body, C – flagellar basal body and surrounding structures.

fbb – flagellar basal body, mct – microtubule, n – nucleus, nu – nucleolus, rf – radial fibrils, rs – reserve substance.

Scale bars: A – 0.5, B – 0.5, C – 0.2 μm .

355



356

357

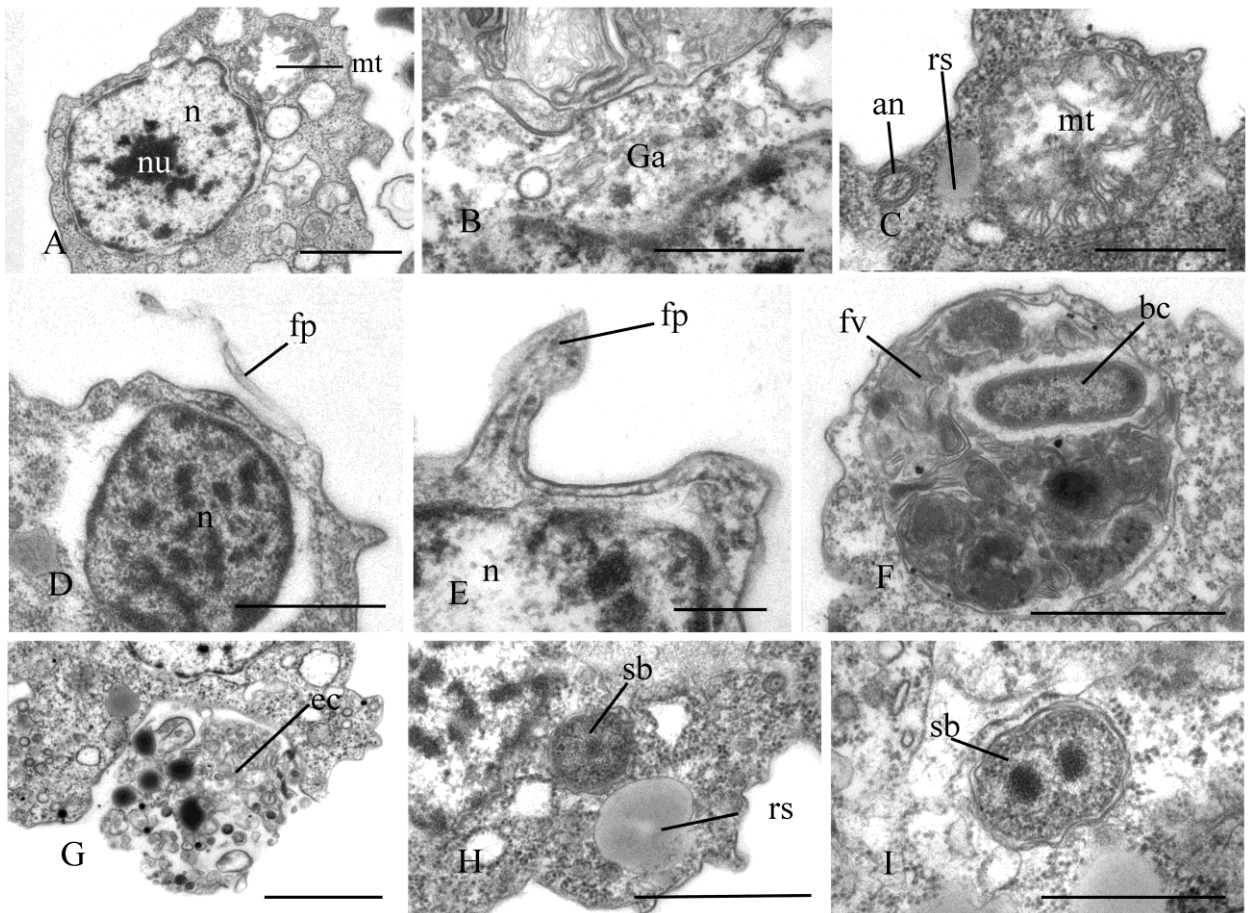
358

359

360

361

Fig. 8. Arrangement of two basal bodies of *Pigoraptor vietnamica* relative to one another. A – F – serial sections of basal bodies. fbb – flagellar basal body, mct – microtubule, n – nucleus, nfbb – non-flagellar basal body. Scale bars: A – F – 0.5 μ m.



362

363

364

365

Fig. 9. Sections of nucleus and other cell structures of *Pigoraptor vietnamica*. A – nucleus, B – Golgi apparatus, C – mitochondrion, D – E – nucleus and filopodia, F – food vacuole, G – exocytosis, H – reserve substance, I – dividing symbiotic bacteria.

366 an – flagellar axoneme, bc – bacterium, ec – ectoproct, fb – filopodium, fv – food vacuole,
367 ga – Golgi apparatus, mt – mitochondrion, n – nucleus, nu – nucleolus, rs – reserve substance, sb
368 – symbiotic bacteria.

369 Scale bars: A – 1, B – 0.5, C – 0.5, D – 0.5, E – 0.2, F – 1, G – 1, H – 1, I – 0.5 μm .

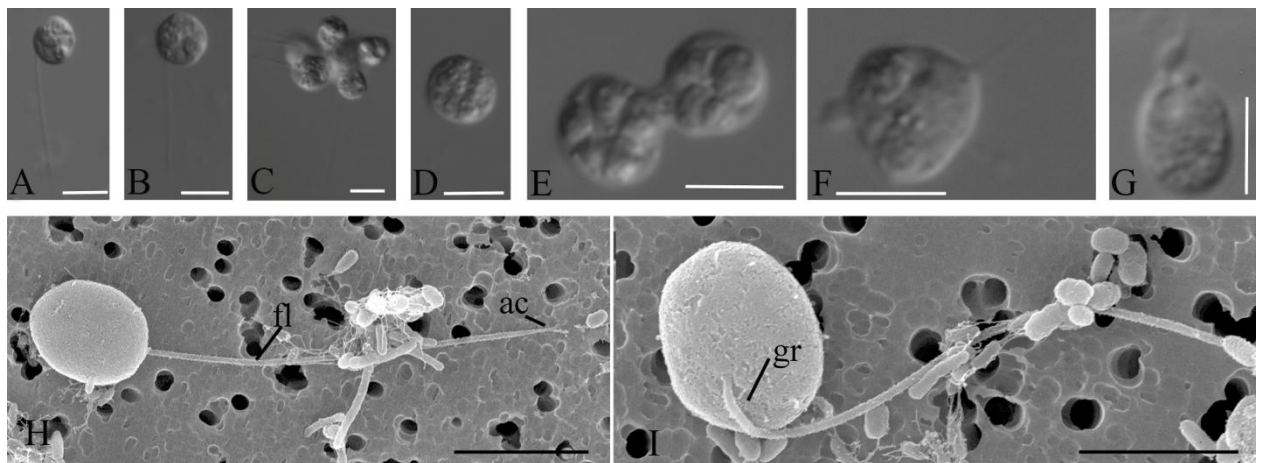
370

371 *Pigoraptor chileana* Tikhonenkov, Hehenberger, Mylnikov et Keeling 2017

372

373 Morphology and life cycle

374 The unflagellated, roundish cells measure 6-14 μm in diameter. The flagellum emerges
375 from a shallow groove and is 8-16 μm in length (Fig. 10 A,B,H,I). The flagellum ends with the
376 acroneme. This species is identical to *Pigoraptor vietnamica* in body plan, movement, feeding,
377 growth conditions, joint feeding and aggregation behaviours (Fig. 10 C, Video 15, 16),
378 encystation (Fig. 10 D), binary division (Fig. 10 E), but additionally characterized by the absence
379 of symbiotic bacteria and much reduced capability to produce filopodia and lobopodia (Fig. 10
380 F,G), which are extremely rare in *Pigoraptor chileana*.



381

382 Fig. 10. External morphology and life forms of *Pigoraptor chileana*. A, B, H, I – general
383 view of flagellated cell (DIC and SEM); C – cell aggregation; D – cyst; E – binary division; F,G
384 – cell with short lobopodia and filipodia.

385 ac – flagella arconeme, gr – groove, fl – flagellum.

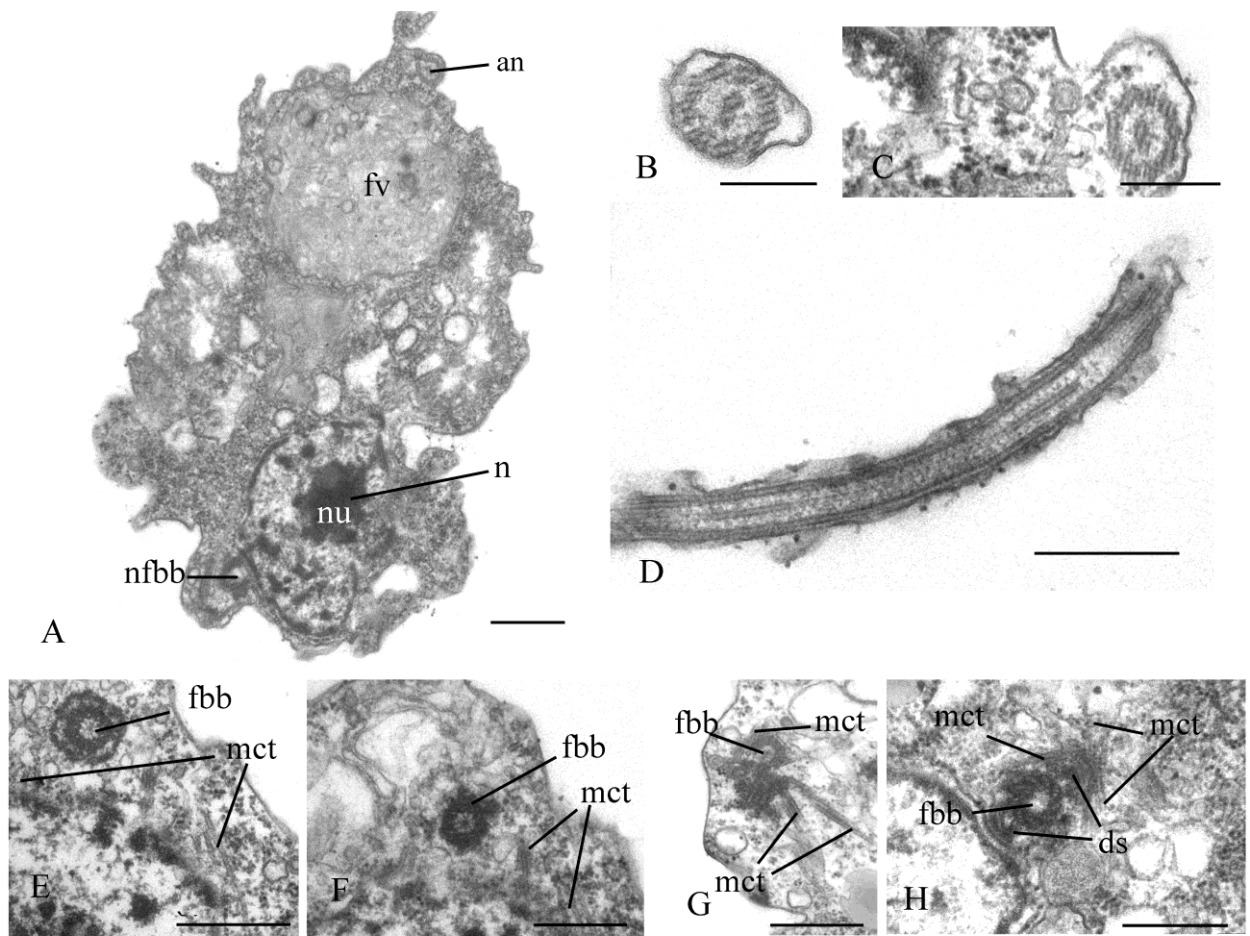
386 Scale bars: A-G – 10, H – 9, I – 4 μm .

387

388 Cell ultrastructure

389 The cell is naked and surrounded by the plasmalemma. The nucleus is positioned close to
390 the posterior cell end (Fig. 11 A). The flagellum is naked and the flagellar axoneme has an
391 ordinary structure (9+2) in section (Fig. 11 B–D). The flagellum can be retracted into the cell
392 which is visible in some sections (Fig. 11 A, C). Flagellar and non-flagellar basal bodies are
393 located near the nucleus (Fig. 11 A) and lie approximately at a 60-90 degrees angle to each other
394 (Fig. 12 A–F). The flagellar basal body contains a wheel-shaped structure in the proximal part
395 (Fig. 11 E,F). Single microtubules and microtubule bundles are situated near this basal body
396 (Fig. 11 E–H). Some microtubules arise from dense spots close to the basal body (Fig. 11 H).

397 Rare, thin, sometimes branching filopodia may contain superficially microtubule-like
398 profiles (Fig. 12 G–I). The roundish nucleus is about 1.5 μm in diameter and has a central
399 nucleolus (Fig. 11A). Chromatin granules are scattered within the nucleoplasm. The Golgi
400 apparatus was not observed. Mitochondria contain lamellar cristae and empty space inside (Fig.
401 13 A, B). Cells usually contain one large food vacuole (Fig. 11A, Fig. 13 C), which contains
402 remnants of eukaryotic prey and bacteria. Storage compounds are represented by roundish
403 (presumably glycolipid) granules 0.2-0.4 μm in diameter (Fig. 13 C). The single ultrathin section
404 of the dividing cell (possible open orthomitosis) was obtained in metaphase stage (Fig. 13 D).
405



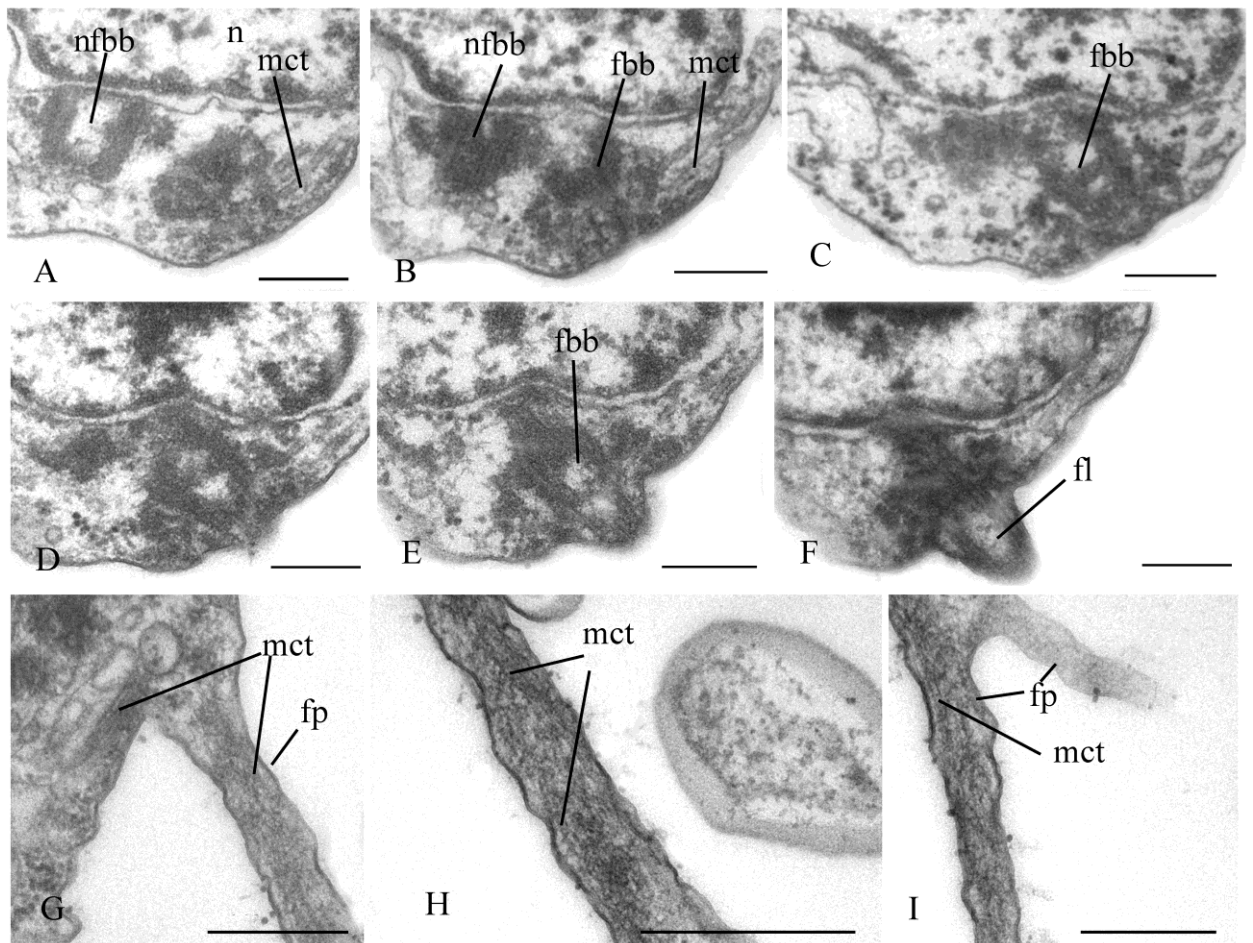
406
407 Fig. 11. General view, flagellum and flagella root system of *Pigoraptor chileana*. A –
408 general view of the cell section. B – D – flagellum, E– H – flagellar basal body and surrounding
409 structures.

410 an – axoneme, ds – dense spot, fbb – flagellar basal body, fv – food vacuole, mct –
411 microtubule, n – nucleus, nfbb – non-flagellar basal body, nu – nucleolus.

412 Scale bars: A – 0.5, B – 0.2, C – 0.2, D – 0.5, E – 0.5, F – 0.5, G – 0.5, H – 0.5 μm .

413
414

415



416

417

418

419

420

421

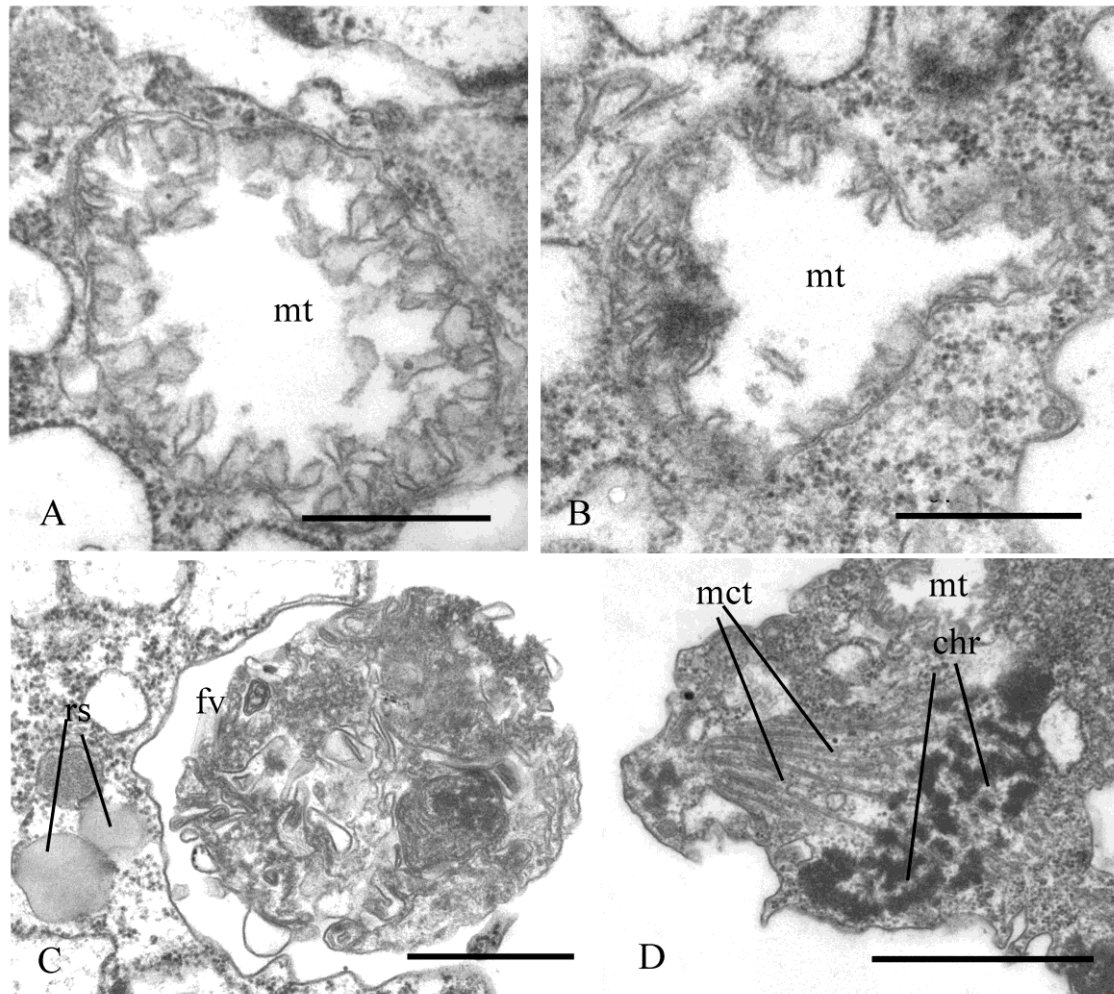
422

Fig. 12. Arrangement of basal bodies and structure of filopodia of *Pigoraptor chileana*. A – F – serial sections of basal bodies, G – I – filipodia.

fbb – flagellar basal body, fl – flagellum, fp – filopodium, mct – microtubule, n – nucleus, nfbf – non-flagellar basal body.

Scale bars: A – F – 0.2, G – I – 0.5 μ m.

423



424

425

426

427

428

429

430

Fig. 13. Mitochondria, food vacuole and nucleus division of *Pigoraptor chileana*. A, B – mitochondria, C – food vacuole and exocytose, D – nucleus division in metaphase stage.

chr – chromosomes, fv – food vacuole, mct – microtubule, mt – mitochondrion, rs – reserve substance.

Scale bars: A – 0.5, B – 0.5, C – 0.5, D – 1 μ m.

431

Key features of novel unicellular opisthokonts and origin of multicellularity in Metazoa

432

433

434

435

436

437

Our understanding of the origin and early evolution of animals has transformed as a result of the study of their most closely related sister groups of unicellular organisms: choanoflagellates, filastereans, and ichthyosporeans (King et al., 2008; Suga et al., 2013; Suga, Ruiz-Trillo, 2013). Our discovery of previously unknown unicellular Holozoa from freshwater bottom sediments in Vietnam and Chile provides new material for analysis.

438

Eukaryotrophy

439

440

441

442

A distinctive feature of all three new species is their feeding on eukaryotic prey of similar or larger size, which is unusual (if not unique) for unicellular Holozoa. While they consume entire prey cells or only the cytoplasmic contents of eukaryotic cells, which resembles the phagocytotic uptake of the contents of *Schistosoma mansoni* sporocysts by the filasterean

443 *Capsaspora owczarzaki* in laboratory conditions (Owczarzak et al., 1980), they can also feed on
444 clusters of bacteria, resembling the phagocytic uptake of bacteria by choanoflagellates (Dayel,
445 King, 2014). It is particularly noteworthy that the organisms we discovered, do not possess
446 extrusive organelles for paralyzing and immobilizing the prey, which is typical for
447 eukaryovorous protists. Our observations show that, prior to absorption, they somehow adhere to
448 the surface of the prey cell. Studies on the choanoflagellate *Monosiga brevicollis* have shown
449 that cadherins, that function as cell-cell adhesion proteins in animals, are located on the
450 microvilli of the feeding collar and colocalize with the actin cytoskeleton (Abedin, King, 2008).
451 *M. brevicollis* is non-colonial, thus suggesting that cadherins participate in prey capture, not
452 colony formation. In addition, studies of the colonial choanoflagellate *Salpingoeca rosetta* did
453 not indicate a role of the cadherins in colony formation, further supporting the notion that
454 cadherins do not play a role in cell-cell adhesion between choanoflagellates, and perhaps also did
455 not in the unicellular ancestor of animals (Seb e-Pedr os et al., 2017). In the case of the unicellular
456 predators *Syssomonas* and *Pigoraptor*, adherence to a large and actively moving prey seems to
457 be crucial for feeding and important for survival. Interestingly, the *Syssomonas* transcriptome
458 does not include cadherin genes, but it does express C-type lectins (carbohydrate-binding
459 proteins performing various functions in animals, including intercellular interaction, immune
460 response and apoptosis). A reverse pattern of gene distribution is seen in *Pigoraptor*, where
461 cadherin domain-containing transcripts were found but no C-type lectins (Hehenberger et al.,
462 2017).

463 The presence of eukaryotrophy as a type of feeding within both filastereans and
464 Pluriformea suggests that predation could be or have once been widespread among unicellular
465 relatives of animals, and perhaps that the ancestor of Metazoa was able to feed on prey much
466 larger than bacteria. The “joint feeding” we observed many times in cultures of *Syssomonas* or
467 *Pigoraptor*, including the behaviour where cells are attracted to the large prey by other predators
468 already feeding on it, is probably mediated by chemical signaling of the initially attached
469 predator cell. The newly arriving cells also adhere to the plasmalemma of the prey, partially
470 merging with each other and sucking out the contents of the large prey cell together. The
471 merging of predator cells during feeding is quite unusual, and may represent a new factor to
472 consider in the emergence of aggregated multicellularity. In addition, putative chemical
473 signaling to attract other cells of its species is observed during the formation of syncytial
474 structures in these species. In this context, alpha and beta-integrins and other components of the
475 so-called integrin adhesome, which are responsible for interaction with the extracellular matrix
476 and the transmission of various intercellular signals, were found in the transcriptomes of all three
477 studied species (Hehenberger et al., 2017).

478

479 ***Starch breakdown by Syssomonas***

480 An interesting phenomenon was observed in clonal cultures of *Syssomonas*, where the
481 predator can completely engulf starch granules of the same size as the cell, also mediating the
482 rapid destruction of rice grains into smaller fragments and individual starch crystals (Fig. S1). It
483 is possible that *Syssomonas* secretes hydrolytic enzymes that provide near-membrane
484 extracellular digestion. Near-membrane extracellular digestion in animals is of great importance
485 for the breakdown of various biopolymers and organic molecules (for example, in the intestinal
486 epithelium of mammals in the zone of limbus strigillatus in the glycocalix layer).

487 This ability of *Syssomonas* to feed on starch is likely promoted by the expression of
488 numerous enzymes that are putatively involved in starch breakdown (several α -amylases and α -
489 glucosidases, a glycogen debranching enzyme and a glycogen phosphorylase) (Table 1). For
490 example, *Syssomonas* has five distinct putative alpha-amylases, one of them not found in any
491 other Holozoa present in our database (Table 1). Similarly, one of the four α -glucosidases in *S.*
492 *multiformis* seems to be specific to this lineage, and possibly the Filasterea, within the Holozoa.
493 While α -amylases and α -glucosidases are able to hydrolyze α -1,4-linked glycosidic linkages,
494 mobilization of the starch molecule at the α -1,6 glycosidic bonds at branch points requires the
495 activity of debranching enzymes. A possible candidate for the catalysis of this reaction is a
496 conserved glycogen debranching enzyme in *S. multiformis*, orthologous to the human *AGL* gene
497 (Table 1). Additionally, we identified a transcript for a glycogen phosphorylase (orthologous to
498 the human *PYGB*, *PYGL* and *PYGM* genes), an enzyme involved in the degradation of large
499 branched glycan polymers.

500 Our observations also show that, in the presence of starch in culture, *Syssomonas* can
501 form resting stages of unidentified genesis, which tend to adhere to each other and to starch
502 grains.

503

504

505

506

507

508

509

510

511

512 Table 1. Transcripts for putative starch-degrading enzymes in *S. multiformis* and the
 513 presence/absence of corresponding orthologs in other unicellular holozoan lineages/Metazoa.
 514 Accession numbers for *S. multiformis* are from the corresponding TransDecoder output files as
 515 described in Hehenberger et al., 2017. Pfam domains used to identify candidates in *S.*
 516 *multiformis* and/or annotated direct human orthologous genes are indicated in brackets in column
 517 1. NA, no direct orthologs recovered in our dataset; +, direct orthologs present in phylogeny; (+)
 518 short fragment of one lineage representative.

	<i>S. multiformis</i>	Ichthyosporea	Filasterea	Choanoflagellates	Metazoa
α-amylases (PF00128)					
1.	Colp12_sorted@267, Colp12_sorted@268, Colp12_sorted@269	+	(+)	+	NA
2.	Colp12_sorted@19603	NA	NA	NA	NA
3.	Colp12_sorted@18987, Colp12_sorted@16467, Colp12_sorted@17178	NA	+	+	+
4.= paralog to 3.	Colp12_sorted@8715	+	+	+	+
5. (<i>SLC3A1</i>)	Colp12_sorted@10150	NA	NA	+	+
α-glucosidases (PF01055)					
1.	Colp12_sorted@9290, Colp12_sorted@22295	NA	(+)	NA	NA
2.	Colp12_sorted@1339, Colp12_sorted@1341	+	+	NA	+
3.= paralog to 2.	Colp12_sorted@9196, Colp12_sorted@14409, Colp12_sorted@18957, Colp12_sorted@21457, Colp12_sorted@31517	+	+	NA	+
4. (<i>GANAB/GANC</i>)	Colp12_sorted@13767	+	+	+	+
glycogen phosphorylase (PYGB/PYGL/PYGM)					
1.	Colp12_sorted@1564	+	+	+	+
glycogen debranching enzyme (AGL)					
1.	Colp12_sorted@14615	+	+	+	+

519
 520
 521
 522
 523
 524
 525

526 ***Structural features***

527 *Syssomonas* and *Pigoraptor* both display a broad morphological plasticity: all three
528 species have a flagellar stage, form pseudopodia and cysts, and can form aggregations of several
529 cells. *Syssomonas multiformis* also has an amoeboid non-flagellar stage. The dominating life
530 form of all three species in culture is the uniflagellar swimming cell. Interestingly, amoeboid and
531 pseudopodial life forms were detected in cultures only after two years of cultivation and
532 observation, suggesting they may be extremely rare in nature. Overall, the morphological
533 differences between cells of the same type of the two genera, *Syssomonas* and *Pigoraptor*, are
534 few and subtle. Given these genera are distantly related within the tree of Holozoa, it is
535 interesting to speculate that they may be the result of morphostasis and by extension retain
536 features resembling those of an ancestral state of holozoan lineages.

537 It has been established that single cells of *Syssomonas* and *Pigoraptor* can temporarily
538 attach themselves to the substrate and, by beating their flagellum, can create water currents to
539 putatively attract food particles, similar to choanoflagellates and sponge choanocytes (Fig. 1 E,
540 Video 2). Choanocytes and choanoflagellates possess, in addition to the flagellum, a collar
541 consisting of cytoplasmic outgrowths reinforced with actin filaments (microvilli) that serve to
542 capture bacterial prey. The thin filopodia that are observed on the cell surface of all three
543 *Syssomonas* and *Pigoraptor* species may thus be homologous to collar microvilli. But this will
544 require further evidence in form of homologous proteins in these structures or evidence of their
545 function in *Syssomonas* and *Pigoraptor*. While the filopodia of *Syssomonas* have no obvious
546 structural contents, the outgrowths of *Pigoraptor* sometimes contain microtubular-like profiles.
547 Cross sections of these structures were not obtained, but they may represent parallel
548 microfilaments such as recently found in the filopodial arms of *Ministeria vibrans* (Mylnikov et
549 al., 2019). The organisation of the *Ministeria* filopodial arms in turn resembles the microvilli of
550 choanoflagellates, which have stable bundles of microfilaments at their base. It has been
551 proposed previously that the ancestor of Filozoa (Filasterea+Choanoflagellida+Metazoa)
552 probably had already developed filose tentacles, which have aggregated into a collar in the
553 common ancestor of choanoflagellates/sponges (Shalchian-Tabrizi et al., 2008), and that
554 microvilli were present in the common ancestor of Filozoa (Mylnikov et al., 2019).

555 A single, posterior flagellum is the defining characteristic of opisthokonts (Cavalier-
556 Smith, Chao, 2003). However, the flagellum has not yet been found in all known Opisthokonta
557 lineages. Torruella et al. (2015) have found several proteins corresponding to key components of
558 the flagellum in *Corallochytrium* and the filose amoeba *Ministeria vibrans*, which have been
559 considered to lack flagella. The authors have shown that the stalk used by *Ministeria* to attach to
560 the substrate is a modified flagellum. Recently, morphological observations on another strain of

561 *Ministeria vibrans* (strain L27; Mylnikov et al., 2019) revealed that this strain lacks the stalk for
562 substrate attachment, but possesses a typical flagellum that projects forward and beats at attached
563 to the substrate cells (see Fig. 2h and Video S1 in Mylnikov et al., 2019). The authors concluded
564 that the filasterean ancestor possessed a flagellum, which was subsequently lost in *Capsaspora*
565 *owczarzaki*. In the case of *Corallochytrium limacisporum*, it was suggested that it has a cryptic
566 flagellate stage in its life cycle (Torruella et al., 2015), as has been proposed for other eukaryotes
567 (*Aureococcus* and *Ostreococcus*, for instance) based on their genome sequences (Wickstead,
568 Gull, 2012). Therefore, the flagellate stage could have been the one morphological trait uniting
569 *Corallochytrium* and *Syssomonas* within “Pluriformea”. Interestingly, the ancestor of
570 ichthyosporeans probably also had a flagellum, which is preserved in the Dermocystida (at the
571 stage of zoospores), but was again lost in the Ichthyophonida.

572 The central filament of the flagellum, which connects the central pair of microtubules
573 with the transversal plate in *Syssomonas* and *Pigoraptor*, is also noteworthy, since this character
574 was previously known only in the choanoflagellates and was considered a unique feature for this
575 lineage. The cone-shaped elevation of the surface membrane around the base of the flagellum in
576 *Syssomonas* was also thought typical for choanoflagellates.

577

578 ***Origins of multicellularity***

579 As mentioned above, numerous theories about the origin of Metazoa exist. One of the
580 first and widely accepted evolutionary theories on the origin of animals is the Gastrea theory of
581 Ernst Haeckel (Haeckel, 1874). Based on the blastula and gastrula stages that various animals
582 undergo during their embryonic development, Haeckel suggested that the first step in the
583 evolution of multicellularity in animals was the formation of a hollow ball, the walls of which
584 consisted of identical flagellated cells, which he called Blastea. This stage is followed by
585 gastrulation, where the ball invaginated, leading to the primary cellular differentiation into ecto-
586 and endoderm. In combination with modern theories, such as the choanoblastea theory, which
587 highlights the similarity between Haeckel's Blastea and the choanoflagellate colony (Nielsen,
588 2008), this model is still the most commonly used explanation for the origin of multicellular
589 animals. An important assumption of the Gastrea theory is that cell differentiation took place
590 only *after* multicellularity arose, suggesting that animals originated from a single cell type. This
591 in turn generated the hypothesis that multicellular animals originated from a choanoflagellate-
592 like colony-forming ancestor (Seb e-Pedr os et al., 2017), supported by the possible homology
593 between sponge choanocytes and choanoflagellates (Adamska, 2016), and is consistent with the
594 idea behind the Haeckel-Muller Biogenetic Law, that ontogenesis recapitulates phylogenesis
595 (Hashimshony et al., 2015).

596 However, there are, for example, some basic differences between sponges and
597 choanoflagellates in how their collar and flagella interact, so, though choanocytes and
598 choanoflagellates are superficially similar, homology should not be automatically assumed (see
599 Mah et al., 2014 for details). More importantly, recent ultrastructural studies on the structure of
600 kinetids (flagellar apparatus) of various sponge choanocytes and choanoflagellates show that
601 they are fundamentally different in many respects (see Pozdnyakov, Karpov, 2016; Pozdnyakov
602 et al., 2017, 2018 for details). These differences are significant, as the kinetid (consisting of the
603 flagella itself, the transition zone, and the kinetosomes with attached microtubular or fibrillar
604 roots) represents one of the very few ultrastructural systems in eukaryotic cells considered a
605 conservative indicator of phylogenetic relationship (Lynn, Small, 1981; Moestrup, 2000; Yubuki
606 and Leander, 2013). Choanocyte kinetids contain more elements that can be considered
607 plesiomorphic for opisthokonts than do choanoflagellate kinetids. For example, significant
608 differences in the spatial arrangement of the non-flagellar basal body, in the structure of the
609 transitional zone and the flagellar root system were found when comparing the flagellate
610 apparatus of the freshwater sponge *Ephydatia fluviatilis* (order Haplosclerida) and the
611 choanoflagellates, but in all of these features the *Ephydatia* choanocyte kinetid is similar to the
612 kinetid of zoospores of chytrids, which are more distantly-related Holomycota (Karpov,
613 Efremova, 1994). Flagellated cells of some ichthyosporeans also possess ultrastructural features in
614 common with flagellated fungi from Holomycota. Therefore, the idea that sponges and by
615 extension all Metazoa descend directly from a single-celled organism similar to
616 choanoflagellates is not supported by the results of the kinetid ultrastructure study (Pozdnyakov
617 et al., 2017).

618 A more detailed understanding of the unicellular relatives of animals has, however, raised
619 an alternative to the Gastrea theory. Specifically, the presence of diverse life forms in complex
620 life cycles and the prevalence of cellular aggregations that bear little similarity to the blastula all
621 suggest that cell *differentiation might have preceded* the origin of the blastula. Moreover,
622 unicellular relatives of animals were shown to contain a variety of genes homologous to those
623 involved in cell adhesion, differentiation and development, and signal transduction in Metazoa.
624 Some of them were considered to be unique to animals (e.g. transcription factors T-box and
625 Rel/NF-kappa B, Crumbs protein, integrin beta) as they were absent in choanoflagellates (the
626 closest relatives of Metazoa), but later they were found to be present in other unicellular Holozoa
627 (Mikhailov et al., 2009; Sebé-Pedrós et al., 2013a; Shalchian-Tabrizi et al., 2008). To date, it is
628 well known that homologues of most genes controlling the development of animals, their cell
629 differentiation, cell-cell and cell-matrix adhesion are present in various lineages of unicellular
630 organisms (King et al., 2003; Sebé-Pedrós et al., 2016; Suga et al., 2013; Williams et al., 2014),

631 which suggests that genetic programs of cellular differentiation and adhesion arose relatively
632 early in the evolution of opisthokonts and before the emergence of multicellularity (King et al.,
633 2003; Ruiz-Trillo et al., 2007; Shalchian-Tabrizi et al., 2008; Mikhailov et al., 2009; Brunet,
634 King, 2018).

635 One specific idea positing that cell differentiation preceded the formation of colonies is
636 the “synzoospore hypothesis” (Sachwatkin, 1956; Zakhvatkin, 1949; and see Mikhailov et al.
637 2009 for details). In brief, three types of cell cycle alternate in the ontogenesis of multicellular
638 animals: monotomy (alternate phases of cell growth and division of somatic cells), hypertrophic
639 growth (in female sex cells) and palintomy (the egg undergoes a series of consecutive divisions).
640 Zakhvatkin noted that some protists alternate between different types of life cycle, and suggested
641 that the unicellular ancestor of Metazoa already had differentiated cells as a result of such a
642 complex life cycle. The life cycle complexity, in turn, results from the fact that monotomic cells
643 are usually sedentary, or at least less mobile, and can change their phenotype (from flagellated to
644 amoeboid, etc.) depending on the environment; the process of palintomy is necessary for the
645 formation of morphologically identical dispersal cells (spores or zoospores). These dispersal
646 cells remain attached to each other, forming a primary flagellated larva — the synzoospore or
647 blastula (cited from Mikhailov et al., 2009).

648 The synzoospore hypothesis is consistent with recent observations of complex life cycles
649 in unicellular opisthokonts possessing cellular differentiation, the presence of sedentary trophic
650 phases, and a tendency to aggregation; as seen in choanoflagellates (Cavalier-Smith, 2017; Dayel
651 et al., 2011; Dayel, King, 2014; Leadbeater, 1983; Maldonado, 2004), filastereans (Sebé-Pedrós
652 et al., 2013b), *Corallochytrium* (Raghukumar, 1987), ichthyosporeans (Arkush et al., 2003;
653 Ruiz-Trillo et al., 2007; Suga, Ruiz-Trillo, 2013), chytridiomycetes (Money, 2016), and
654 nucleariid amoebae (Smirnov, 2000). According to this theory, multicellularity in animals arose
655 through the temporal integration of various types of cells, which were already present in
656 different parts of the life cycle. The hypothetical ancestor of animals in this model would thus
657 already have genetic programs for cell differentiation (including cadherins, integrins, tyrosine
658 kinases).

659 Developing the synzoospore hypothesis further, Mikhailov et al. (2009) proposed an
660 evolutionary mechanism of “*transition from temporal to spatial cell differentiation*” to explain
661 the emergence of multicellular animals. In this model, the ancestor of Metazoa was a sedentary
662 colonial protist filter-feeder with colonies formed by cells of different types, which arose
663 because filtration efficiency is significantly enhanced through the cooperation of cells of
664 different types. Dispersal cells produced by the sedentary stage, the zoospores, remained
665 attached together in early metazoans (which increased survivability) as a synzoospore to form a

666 primary larva, the blastula. Development of a whole colony from such a multicellular larva
667 occurred through the *differentiation of genetically identical* zoospore cells. This was critical for
668 the maintenance of long-term cell adhesion and thus emergence of true multicellularity, as
669 opposite to temporary colonies and aggregations composed of genetically heterogeneous cells.
670 The authors suggest that the dispersal stages of the sedentary trophic body — primary blastula-
671 like larvae – acquired adaptations to the predatory lifestyle, which triggered the development of
672 primary intestine, muscular and nervous systems (Mikhailov et al., 2009).

673 The origin of multicellularity can in this view be seen as a *transition from temporal to*
674 *spatiotemporal cell differentiation* (Sebé-Pedrós et al., 2017). In a unicellular ancestor of
675 Metazoa that was a sexually reproducing bacteriotroph with many differentiated, temporally-
676 separated cells, the transitions between different cell states would be regulated by expression of
677 transcription factor families in response to environmental conditions such as availability of
678 nutrients or preferred bacterial food. These temporally-regulated cell types then became spatially
679 integrated, existing simultaneously but in different parts of a now multicellular conglomerate
680 with different cell types carrying out different functions. Further diversification could then be
681 accompanied by the evolution of additional mechanisms for complex gene regulation networks
682 involving signaling pathways, expansion of transcription factors, and the evolution of new
683 genomic regulatory mechanisms to control spatial differentiation of existing genetic modules
684 specific to a particular cell type. At that point, the life cycle of the protozoan ancestor of animals
685 probably included one or more clonal and/or aggregative multicellular stages (Sebé-Pedrós et al.,
686 2017).

687 To distinguish between the models for the origin of animal multicellularity, genomics
688 alone is not sufficient, and data on morphology, life cycle, and structural features of basal
689 holozoans is also needed. From the current analysis, all three novel species of unicellular
690 Holozoa have life histories that are consistent with major elements of the synzoospore model
691 (see Fig. 3A in Mikhailov et al., 2009 and Fig. 5a,b in Sebé-Pedrós et al., 2017). Specifically,
692 these organisms have complex life histories characterized by a variety of forms: flagellates,
693 amoebae, amoeboflagellates, cysts. All three species have the tendency to form aggregations.
694 *Syssomonas* possesses both clonal and aggregative multicellular stages, as predicted for the
695 ancestor of animals. Moreover, the formation of aggregations can be associated with feeding on
696 large eukaryotic prey, but also by cysts, which can adhere to each other and to starch grains in
697 culture and divide multiply. Both these probably require cellular signaling. Eating a large
698 eukaryotic prey, sometimes exceeding the size of a predator, also leads to hypertrophic cell
699 growth (described as proliferative stage in Sebé-Pedrós et al., 2017) with a subsequent phase of
700 palintomic division (in *Syssomonas*). All these characters are predicted by the synzoospore

701 model. Interestingly, many of these are apparently triggered by the behaviour of feeding on large
702 eukaryotic prey, highlighting this as is an interesting and potentially powerful trigger in general
703 for the formation and development of aggregates (e.g., joint feeding) and clonal multicellularity
704 (e.g., hypertrophic growth followed by palintomy), perhaps playing a role in the origin of
705 multicellularity in ancestors of Metazoa.

706

707 **Concluding remarks**

708 As we acquire more information about the biology of known unicellular relatives of
709 animals, and even more importantly, describe diverse new species of unicellular Holozoa, more
710 reliable models for the evolutionary histories of specific characteristics that contributed to the
711 emergence of multicellularity in animals are possible. *Syssomonas* and *Pigoraptor* are
712 characterized by complex life cycles, the formation of multicellular aggregations, and an unusual
713 diet for single-celled opisthokonts (partial cell fusion and joint sucking of large eukaryotic prey),
714 all of these features providing new insights into the origin of multicellularity in Metazoa.

715 Genomic and transcriptome analysis of unicellular relatives of animals have shown that
716 genes encoding proteins for cellular signaling and adhesion, as well as genes for embryonic
717 development of multicellular organisms, arose before the emergence of multicellular animals
718 (King et al., 2003; Ruiz-Trillo et al., 2007; Shalchian-Tabrizi et al., 2008; Hehenberger et al.,
719 2017). While these genes almost certainly have slightly different functions in protists than in
720 animals, they nevertheless probably relate to the ability to recognize the cells of their own
721 species, prey, or organic molecules and contribute to the formation of multicellular aggregations,
722 thus increasing the organism's ability to adapt to environmental change. As we learn more about
723 the natural history and behaviour of these organisms, the importance of these processes becomes
724 even more clear. The ancestor of Metazoa probably formed cells of various types that could
725 aggregate and had molecular mechanisms of cell differentiation and adhesion related to those
726 processes. Therefore, cellular differentiation likely arose before the emergence of
727 multicellularity.

728 The feeding modes of the ancestral metazoan may also have been more complex than
729 previously thought, including not only bacterial prey, but also larger eukaryotic cells and organic
730 structures. Indeed, the ability to feed on large eukaryotic prey could have been a powerful trigger
731 in the formation and development both aggregative and clonal multicellular stages that played
732 important roles in the emergence of multicellularity in animals. Lastly, we wish to point out that
733 other new and deep lineages of opisthokonts undoubtedly exist that have not yet been described,
734 and each of these will play an important role in the development of hypotheses on the origin of
735 multicellular animals in future.

736 **Materials and Methods**

737 Novel unicellular opisthokont predators were found in freshwater biotopes in Vietnam
738 and Chile. *Syssomonas multiformis* (clone Colp-12) was obtained from the sample of freshwater
739 pool (11°23'08.0"N, 107°21'44.9"E; T = 39°C; pH = 7.18; DO (ppm) = 0.64; conductivity
740 ($\mu\text{S}/\text{cm}$) = 281; TDS (ppm) = 140), Tà Lài, Cát Tiên National Park, Dong Nai Province, S.R.
741 Vietnam on April 29, 2013. *Pigoraptor vietnamica* (clone Opistho-1) was obtained from
742 freshwater Lake Dak Minh, silty sand on the littoral (12°54'50"N, 107°48'26"E; T = 27 °C;
743 pH=7.03; DO (ppm) = 7.43; conductivity ($\mu\text{S}/\text{cm}$) = 109; TDS (ppm) = 54), Dak Lak Province,
744 S.R. Vietnam on March 26 2015. *Pigoraptor chileana* (clone Opistho-2) was obtained from the
745 bottom sediments of freshwater temporary water body (submerged meadow, 54°02'29.7"S,
746 68°55'18.3"W; T = 16.5°C; pH = 6.62; conductivity ($\mu\text{S}/\text{cm}$) = 141; TDS (ppm) = 72) near the
747 Lake Lago Blanca, Tierra del Fuego, Chile on November 4, 2015.

748 The samples were examined on the third, sixth and ninth days of incubation in accordance
749 with methods described previously (Tikhonenkov et al., 2008). Following isolation by glass
750 micropipette, freshwater clones Colp-12, Opistho-1, and Opistho-2 were propagated on the
751 bodonid *Parabodo caudatus* (strain BAS-1, IBIW RAS) grown in Pratt's medium or spring
752 water (Aqua Minerale, PepsiCo, Moscow Region, Russia or PC Natural Spring Water,
753 President's Choice, Toronto, Canada) by using the bacterium *Pseudomonas fluorescens* as food
754 (Tikhonenkov et al., 2014). The clone Colp-12 was perished after five years of cultivation. The
755 clones Opistho-1 and Opistho-2 are stored in the "Live culture collection of free-living amoebae,
756 heterotrophic flagellates and heliozoans" at the Institute for Biology of Inland Waters, Russian
757 Academy of Science.

758 Light microscopy observations were made by using the Zeiss Axio Scope A.1 equipped
759 with a DIC contrast water immersion objective (63x). The images were taken with the AVT
760 HORN MC-1009/S analog video camera and directly digitized by using the Behold TV 409 FM
761 tuner. Cells with engulfed starch granules were inspected by epifluorescence microscopy after
762 DAPI staining using the Zeiss Axioplan 2 Imaging microscope.

763 For transmission electron microscopy (TEM), cells were centrifuged, fixed at 1 °C for 15-
764 60 min in a cocktail of 0.6% glutaraldehyde and 2% OsO₄ (final concentration) prepared using a
765 0.1 M cacodylate buffer (pH 7.2). Fixed cells were dehydrated in alcohol and acetone series (30,
766 50, 70, 96, and 100%, 20 minutes in each step). Afterward, the cells were embedded in a mixture
767 of Araldite and Epon (Luft, 1961). Ultrathin sections were prepared with an LKB
768 ultramicrotome (Sweden) and observed by using the JEM 1011 transmission electron
769 microscope (JEOL, Japan).

770 For scanning electron microscopy (SEM), cells from exponential growth phase were fixed
771 as for TEM but only for 10 min at 22 °C and gently drawn onto a polycarbonate filter (diameter
772 24 mm, pores 0.8 µm). Following the filtration, the specimens were taken through a graded
773 ethanol dehydration and acetone, and finally put into a chamber of a critical point device for
774 drying. Then dry filters with fixed specimens were mounted on aluminum stubs, coated with
775 gold-palladium, and observed with a JSM-6510LV scanning electron microscope (JEOL, Japan).

776 Analysis of enzymes involved in starch breakdown was based on transcriptomic data
777 obtained as described earlier (Hehenberger et al., 2017). To identify candidates putatively
778 involved in starch breakdown, we used the results of a previous hmmscan analysis of *S.*
779 *multiformis* (Hehenberger et al., 2017) to search for Pfam domains present in known starch-
780 degrading enzymes/enzyme families, such as α -amylases (PF00128), glycoside hydrolase
781 families containing α -glucosidases (PF02056, PF01055, PF03200, PF10566), α -glucan water
782 dikinase 1 (*GWD1*, PF01326), phosphoglucan phosphatase (*DSP4*, PF00782 and PF16561),
783 disproportionating enzymes (PF02446) and pullulanases (PF17967). Additionally, we submitted
784 the *S. multiformis* sorted transcriptome to the KEGG Automatic Annotation Server (KAAS)
785 (Kanehisa et al., 2014) for functional annotation and investigated the output for transcripts
786 involved in starch metabolism. All candidates were investigated using phylogenetic
787 reconstruction. Briefly, they were used as queries in a BLASTp search (e-value threshold 1e-5)
788 against a comprehensive custom database containing representatives of all major eukaryotic
789 groups and RefSeq data from all bacterial phyla at NCBI (<https://www.ncbi.nlm.nih.gov/>, last
790 accessed December 2017) (Altschul et al., 1990). The database was subjected to CD-HIT with a
791 similarity threshold of 85% to reduce redundant sequences and paralogs (Li and Godzik, 2006).
792 Results from blast searches were parsed for hits with a minimum query coverage of 50% and e-
793 values of less than 1e-5. The number of bacterial hits was restrained to 20 hits per phylum (for
794 FCB group, most classes of Proteobacteria, PVC group, Spirochaetes, Actinobacteria,
795 Cyanobacteria (unranked) and Firmicutes) or 10 per phylum (remaining bacterial phyla) as
796 defined by NCBI taxonomy. Parsed hits were aligned with MAFFT v. 7.212, using the—auto
797 option, poorly aligned regions were eliminated using trimAl v.1.2 with a gap threshold of 80%
798 (Katoh and Standley, 2013; Capella-Gutiérrez et al., 2009). Maximum likelihood tree
799 reconstructions were then performed with FastTree v. 2.1.7 using the default options (Price et al.,
800 2010). Phylogenies with overlapping taxa were consolidated by combining the parsed hits of the
801 corresponding queries, removing duplicates and repeating the alignment, trimming and tree
802 reconstruction steps as described above.

803

804

805 **Acknowledgements**

806 We thank Kristina I. Prokina for sample collection in Chile, Dr. Hoan Q. Tran and Tran
807 Duc Dien for assistance with sample collection and trip management in Vietnam, Jürgen F.H.
808 Strassert for help with DAPI staining, and Vladimir V. Aleshin and Kirill V. Mikhailov for
809 fruitful discussion on different aspects of origin of Metazoa. Field work in Vietnam is part of the
810 project “Ecolan 3.2” of the Russian-Vietnam Tropical Centre.

811 **Funding:** This work was supported by the Russian Science Foundation (grant no. 18-14-
812 00239).

813 **Competing interests:** None declared.

814 **References**

- 815 Abedin M, King N. 2008. The premetazoan ancestry of cadherins. *Science* **319**:946–948.
816 doi:10.1126/science.1151084
- 817 Adamska M. 2016. Sponges as models to study emergence of complex animals. *Curr Opin*
818 *Genet Dev* **39**:21–28. doi:10.1016/j.gde.2016.05.026
- 819 Aleshin VV, Konstantinova AV, Mikhailov KV, Nikitin MA, Petrov NB. 2007. Do we need
820 many genes for phylogenetic inference? *Biochemistry Mosc* **72**:1313–1323.
821 doi:10.1134/S000629790712005X
- 822 Altschul, S.F., Gish, W., Miller, W., Myers, E.W., and Lipman, D.J. 1990. Basic local alignment
823 search tool. *J. Mol. Biol.* **215**, 403–410.
- 824 Arkush KD, Mendoza L, Adkison MA, Hedrick RP. 2003. Observations on the life stages of
825 *Sphaerothecum destruens* n. g., n. sp., a mesomycetozoean fish pathogen formally referred
826 to as the rosette agent. *J Eukaryot Microbiol* **50**:430–438. doi:10.1111/j.1550-
827 7408.2003.tb00269.x
- 828 Brown MW, Spiegel FW, Silberman JD. 2009. Phylogeny of the “forgotten” cellular slime mold,
829 *Fonticula alba*, reveals a key evolutionary branch within Opisthokonta. *Mol Biol Evol*
830 **26**:2699–2709. doi:10.1093/molbev/msp185
- 831 Brown MW, Kolisko M, Silberman JD, Roger AJ. 2012. Aggregative multicellularity evolved
832 independently in the eukaryotic supergroup Rhizaria. *Curr Biol* **22**:1123–1127.
833 doi:10.1016/j.cub.2012.04.021
- 834 Brunet T, King N. 2017. The origin of animal multicellularity and cell differentiation. *Dev Cell*
835 **43**:124–140. doi:10.1016/j.devcel.2017.09.016
- 836 Capella-Gutiérrez, S., Silla-Martínez, J.M., and Gabaldón, T. 2009. trimAl: a tool for automated
837 alignment trimming in large-scale phylogenetic analyses. *Bioinformatics* **25**, 1972–1973.

- 838 Cavalier-Smith T. 2017. Origin of animal multicellularity: precursors, causes, consequences –
839 the choanoflagellate/sponge transition, neurogenesis and the Cambrian explosion. *Philos*
840 *Trans R Soc Lond B Biol Sci* **372**:20150476. doi:10.1098/rstb.2015.0476
- 841 Cavalier-Smith T, Chao EE. 2003. Phylogeny of Choanozoa, Apusozoa, and other Protozoa and
842 early eukaryote megaevolution. *J Mol Evol* **56**:540–563. doi:10.1007/s00239-002-2424-z
- 843 Carr M, Richter DJ, Fozouni P, Smith YJ, Jeuck A, Leadbeater BSC, Nitsche F. 2017. A six-
844 gene phylogeny provides new insights into choanoflagellate evolution. *Mol Phylogenet*
845 *Evol* **107**:166–178. doi:10.1016/j.ympev.2016.10.011
- 846 Dayel MJ, King N, 2014. Prey capture and phagocytosis in the choanoflagellate *Salpingoeca*
847 *rosetta*. *PLoS ONE* **9**:e95577. doi:10.1371/journal.pone.0095577
- 848 Dayel MJ, Agelado RA, Fairclough SR, Levin TC, Nichols SA, McDonald K, King N. 2011.
849 Cell differentiation and morphogenesis in the colony-forming choanoflagellate
850 *Salpingoeca rosetta*. *Dev Biol* **357**:73–82. doi:10.1016/j.ydbio.2011.06.003
- 851 del Campo J, Ruiz-Trillo I. 2013. Environmental survey meta-analysis reveals hidden diversity
852 among unicellular opisthokonts. *Mol Biol Evol* **30**:802–805. doi:10.1093/molbev/mst006
- 853 Dunn CW, Hejnol A, Matus DQ, Pang K, Browne WE, Smith SA, Seaver E, Rouse GW, Obst
854 M, Edgecombe GD, Sørensen MV, Haddock SH, Schmidt-Rhaesa A, Okusu A, Kristensen
855 RM, Wheeler WC, Martindale MQ, Giribet G. 2008. Broad phylogenomic sampling
856 improves resolution of the animal tree of life. *Nature* **452**:745–749.
857 doi:10.1038/nature06614
- 858 Feuda R, Dohrmann M, Pett W, Philippe H, Rota-Stabelli O, Lartillot N, Wörheide G, Pisani D.
859 2017. Improved modeling of compositional heterogeneity supports sponges as sister to all
860 other animals. *Curr Biol* **27**:3864–3870.e4. doi:10.1016/j.cub.2017.11.008
- 861 Gobert GN, Stenzel DJ, McManus DP, Jones MK. 2003. The ultrastructural architecture of the
862 adult *Schistosoma japonicum* tegument. *Int J Parasitol* **33**:1561–1575. doi:10.1016/S0020-
863 7519(03)00255-8
- 864 Haeckel E. 1874. Die Gastraea-Theorie, die phylogenetische Klassifikation des Thierreichs und
865 die Homologie der Keimblätter. *Jenaische Z Naturwiss* **8**:1–55. (in German).
- 866 Hashimshony T, Feder M, Levin M, Hall BK, Yanai I. 2015. Spatiotemporal transcriptomics
867 reveals the evolutionary history of the endoderm germ layer. *Nature* **519**:219–222.
868 doi:10.1038/nature13996
- 869 Hehenberger E, Tikhonenkov DV, Kolisko M, del Campo J, Esaulov AS, Mylnikov AP, Keeling
870 PJ. 2017. Novel freshwater predators reshape holozoan phylogeny and reveal the presence
871 of a two-component signalling system in the ancestor of animals. *Curr Biol* **27**:2043–2050.
872 doi:10.1016/j.cub.2017.06.006

- 873 Hertel LA, Bayne CJ, Loker ES. 2002. The symbiont *Capsaspora owczarzaki*, nov. gen. nov. sp.,
874 isolated from three strains of the pulmonate snail *Biomphalaria glabrata* is related to
875 members of the Mesomycetozoea. *Int J Parasitol* **32**:1183–1191. doi:10.1016/s0020-
876 7519(02)00066-8.
- 877 Ivanov AV. 1968. Origin of multicellular animals. Phylogenetic essays. Leningrad: Nauka. 287
878 p. (in Russian).
- 879 James-Clark H. 1866. Note on the *Infusoria flagellata* and the *Spongiae ciliatae*. *Am. J. Sci*
880 **1**:113–114.
- 881 Kanehisa M, Goto S, Sato Y, Kawashima M, Furumichi M, Tanabe M. 2014. Data, information,
882 knowledge and principle: back to metabolism in KEGG. *Nucleic Acids Res.* **42**:D199–
883 D205.
- 884 Karpov SA, Efremova SM. 1994. Ultrathin structure of the flagellar apparatus in the choanocyte
885 of the sponge *Ephydatia fluviatilis*. *Tsitologia* **36**:403–408 (in Russian)
- 886 Katoh, K., and Standley, D.M. 2013. MAFFT multiple sequence alignment software version 7:
887 improvements in performance and usability. *Mol. Biol. Evol.* **30**, 772–780.
- 888 King N, Hittinger CT, Carroll SB. 2003. Evolution of key cell signaling and adhesion protein
889 families predates animal origins. *Science* **301**:361–363. doi:10.1126/science.1083853
- 890 King N, Westbrook MJ, Young SL, Kuo A, Abedin M, Chapman J, Fairclough S, Hellsten U,
891 Isogai Y, Letunic I, Marr M, Pincus D, Putnam N, Rokas A, Wright KJ, Zuzow R, Dirks
892 W, Good M, Goodstein D, Lemons D, Li W, Lyons JB, Morris A, Nichols S, Richter DJ,
893 Salamov A, Sequencing JG, Bork P, Lim WA, Manning G, Miller WT, McGinnis W,
894 Shapiro H, Tjian R, Grigoriev IV, Rokhsar D. 2008. The genome of the choanoflagellate
895 *Monosiga brevicollis* and the origin of metazoans. *Nature* **451**:783–788.
896 doi:10.1038/nature06617
- 897 Lang BF, O'Kelly C, Nerad T, Gray MW, Burger G. 2002. The closest unicellular relatives of
898 animals. *Curr Biol* **12**:1773–1778. doi:10.1016/S0960-9822(02)01187-9
- 899 Leadbeater BSC. 1983. Life-history and ultrastructure of a new marine species of
900 *Proterospongia* (Choanoflagellida). *J Mar Biol Assoc UK* **63**:135–160.
901 doi:10.1017/S0025315400049857
- 902 Leys SP, Cheung E, Boury-Esnaulty N. 2006. Embryogenesis in the glass sponge *Oopsacas*
903 *minuta*: formation of syncytia by fusion of blastomeres. *Integr Comp Biol* **46**:104–117.
904 doi:10.1093/icb/icj016
- 905 Li, W., and Godzik, A. 2006. Cd-hit: a fast program for clustering and comparing large sets of
906 protein or nucleotide sequences. *Bioinformatics* **22**, 1658–1659.

- 907 Lynn DH, Small EB. 1981. Protist kinetids: structural conservatism, kinetid structure, and
908 ancestral states. *Biosystems* **14**:377–385. doi:10.1016/0303-2647(81)90044-7
- 909 Mah JL, Christensen-Dalsgaard KK, Leys S.P. 2014. Choanoflagellate and choanocyte collar-
910 flagellar systems and the assumption of homology. *Evolution and Development* **16**:25–37.
911 doi:10.1111/ede.12060.
- 912 Maldonado M. 2004. Choanoflagellates, choanocytes, and animal multicellularity. *Invertebr Biol*
913 **123**:1–22. doi:10.1111/j.1744-7410.2004.tb00138.x
- 914 Maloof AC, Rose CV, Beach R, Samuels BM, Calmet CC, Erwin DH, Poirier GR, Yao N,
915 Simons FJ. 2010. Possible animal-body fossils in pre-Marinoan limestones from South
916 Australia. *Nat Geosci* **3**:653–659. doi:10.1038/ngeo934
- 917 Medina M, Collins AG, Taylor JW, Valentine JW, Lipps JH, Amaral-Zettler L, Sogin ML. 2003.
918 Phylogeny of Opisthokonta and the evolution of multicellularity and complexity in Fungi
919 and Metazoa. *J Astrobiol* **2**:203–211. doi:10.1017/S1473550403001551
- 920 Mikhailov KV, Konstantinova AV, Nikitin MA, Troshin PV, Rusin LY, Lyubetsky VA, Panchin
921 YV, Mylnikov AP, Moroz LL, Kumar S, Aleoshin VV. 2009. The origin of Metazoa: a
922 transition from temporal to spatial cell differentiation. *Bio Essays* **31**:758–768.
923 doi:10.1002/bies.200800214
- 924 Moestrup Ø. 2000. The flagellate cytoskeleton: Introduction of a general terminology for
925 microtubular roots in protists. In: Leadbeater BS, Green JC, editors. *The Flagellates: Unity,*
926 *Diversity and Evolution*. London: Taylor & Francis. pp 69–94.
- 927 Money NP. 2016. Fungal Diversity. In: *The Fungi (Third Edition)*. Eds: Watkinson SC, Boddy
928 L, Money NP. Elsevier. pp. 1–36.
- 929 Moroz LL, Kocot KM, Citarella MR, Dosung S, Norekian TP, Povolotskaya IS, Grigorenko AP,
930 Dailey C., Berezikov E, Buckley KM, Ptitsyn A, Reshetov D, Mukherjee K, Moroz TP,
931 Bobkova E, Yu F, Kapitonov VV, Jurka J, Bobkov YV, Swore JJ, Girardo DO, Fodor A,
932 Gusev F, Sanford R, Bruders R, Kittler E, Mills CE, Rast JP, Derelle R, Solovyev VV,
933 Kondrashov FA, Swalla BJ, Sweedler JV, Rogaev EI, Halanych KM, Kohn AB. 2014. The
934 ctenophore genome and the evolutionary origins of neural systems. *Nature* **510**: 109–
935 114. doi: 10.1038/nature13400.
- 936 Mylnikov AP, Tikhonenkov DV, Karpov SA, Wylezich C. 2019. Microscopical studies on
937 picoplanctonic *Ministeria vibrans* Tong, 1997 (Filasterea) highlights the cytoskeletal
938 structure of the common ancestor of Filasterea, Metazoa and Choanoflagellata. *Protist*.
939 doi.org/10.1016/j.protis.2019.07.001
- 940 Nielsen C. 1987. Structure and function of metazoan ciliary bands and their phylogenetic
941 significance. *Acta Zoolog* **68**:205–262. doi:10.1111/j.1463-6395.1987.tb00892.x

- 942 Nielsen C. 2008. Six major steps in animal evolution: are we derived sponge larvae? *Evol Dev*
943 **10**:241–257. doi:10.1111/j.1525-142X.2008.00231.x
- 944 Owczarzak A, Stibbs HH, Bayne CJ. 1980. The destruction of *Schistosoma mansoni* mother
945 sporocysts in vitro by amoebae isolated from *Biomphalaria glabrata*: an ultrastructural
946 study. *J Invertebr Pathol* **35**:26–33. doi:10.1016/0022-2011(80)90079-8
- 947 Philippe H, Derelle R, Lopez P, Pick K, Borchiellini C, Boury-Esnault N, Vacelet J, Renard E,
948 Houliston E, Quéinnec E, Da Silva C, Wincker P, Le Guyader H, Leys S, Jackson DJ,
949 Schreiber F, Erpenbeck D, Morgenstern B, Wörheide G, Manuel M. 2009. Phylogenomics
950 revives traditional views on deep animal relationships. *Curr Biol* **19**:706–712.
951 doi:10.1016/j.cub.2009.02.052
- 952 Pozdnyakov IR, Karpov SA. 2016. Kinetid Structure in Choanocytes of Sponges
953 (Heteroscleromorpha): Toward the Ancestral Kinetid of Demospongiae. *J Morph* **277**:925–
954 934. doi:10.1002/jmor.20546
- 955 Pozdnyakov IR, Sokolova AM, Ereskovsky AV, Karpov SA. 2017. Kinetid structure of
956 choanoflagellates and choanocytes of sponges does not support their close relationship.
957 *Protistology* **11**:248–264. doi:10.21685/1680-0826-2017-11-4-6
- 958 Pozdnyakov IR, Sokolova AM, Ereskovsky AV, Karpov SA. 2018. Kinetid structure in sponge
959 choanocytes of Spongillida and Scopalinida in the light of evolutionary relationships
960 within Demospongiae. *Zool J Linnean Soc* **184**:255–272 doi:10.1093/zoolinnean/zlx109
- 961 Price, M.N., Dehal, P.S., and Arkin, A.P. 2010. FastTree 2—approximately maximum-likelihood
962 trees for large alignments. *PLoS ONE* **5**, e9490.
- 963 Raghukumar S. 1987. Occurrence of the Thraustochytrid, *Corallochytrium limacisporum* gen. et
964 sp. nov. in the coral reef lagoons of the Lakshadweep Islands in the Arabian Sea. *Bot Mar*
965 **30**:83–89. doi:10.1515/botm.1987.30.1.83
- 966 Ratcliff WC, Denison RF, Borrello M, Travisano M. 2012. Experimental evolution of
967 multicellularity. *Proc Nat Acad Sci USA* **109**:1595–1600. doi:10.1073/pnas.1115323109
- 968 Ruiz-Trillo I, Burger G, Holland PW, King N, Lang BF, Roger AJ, Gray MW. 2007. The origins
969 of multicellularity: a multi-taxon genome initiative. *Trends Genet* **23**:113–118.
970 doi:10.1016/j.tig.2007.01.005
- 971 Ruiz-Trillo I, Roger AJ, Burger G, Gray MW, Lang BF. 2008. A phylogenomic investigation
972 into the origin of metazoa. *Mol Biol Evol* **25**:664–672. doi:10.1093/molbev/msn006
- 973 Ryan JF, Pang K, Schnitzler CE, Nguyen AD, Moreland RT, Simmons DK, Koch BJ, Francis
974 WR, Havlak P, NISC Comparative Sequencing Program, Smith SA, Putnam NH, Haddock
975 SH, Dunn CW, Wolfsberg TG, Mullikin JC, Martindale MQ, Baxevanis AD. 2013. The

- 976 genome of the ctenophore *Mnemiopsis leidyi* and its implications for cell type evolution.
977 *Science* **342**:1242592. doi:10.1126/science.1242592
- 978 Sachwatkin AA. 1956. Vergleichende embryologie der niederen wirbellosen: ursprung und
979 gestaltungswege der individuellen entwicklung der vielzeller. Berlin: VEB Deutscher
980 Verlag der Wissenschaften. S. 401.
- 981 Schierwater B, Eitel M, Jakob W, Osigus H-J, Hadrys H, Dellaporta SL, Kolokotronis S-O, De
982 Salle R. 2009. Concatenated analysis sheds light on early metazoan evolution and fuels a
983 modern “Urmetazoon” hypothesis. *PLoS Biol* **7**:e1000020.
984 doi:10.1371/journal.pbio.1000020
- 985 Sebé-Pedrós A, Ariza-Cosano A, Weirauch MT, Leininger S, Yang A, Torruella G, Adamski M,
986 Adamska M, Hughes TR, Gómez-Skarmeta JL, Ruiz-Trillo I. 2013a. Early evolution of the
987 T-box transcription factor family. *Proc Natl Acad Sci USA* **110**:16050–16055.
988 doi:10.1073/pnas.1309748110
- 989 Sebé-Pedrós A, Irimia M, Del Campo J, Parra-Acero H, Russ C, Nusbaum C, Blencowe BJ,
990 Ruiz-Trillo I. 2013b. Regulated aggregative multicellularity in a close unicellular relative
991 of metazoan. *eLife* **2**:e01287. doi:10.7554/eLife.01287
- 992 Sebé-Pedrós A, Peña MI, Capella-Gutiérrez S, Antó M, Gabaldón T, Ruiz-Trillo I, Sabido E.
993 2016. High-throughput proteomics reveals the unicellular roots of animal
994 phosphosignaling and cell differentiation. *Dev Cell* **39**:186–197.
995 doi:10.1016/j.devcel.2016.09.019
- 996 Sebé-Pedrós A, Degnan BM, Ruiz-Trillo I. 2017. The origin of Metazoa: a unicellular
997 perspective. *Nat Rev Genet* **18**:498–512. doi:10.1038/nrg.2017.21
- 998 Shalchian-Tabrizi K, Minge MA, Espelund M, Orr R, Ruden T, Jakobsen KS, Cavalier-Smith T.
999 2008. Multigene phylogeny of choanozoa and the origin of animals. *PLoS ONE* **3**:e2098.
1000 doi:10.1371/journal.pone.0002098
- 1001 Sharpe SC, Eme L, Brown MW, Roger AJ. 2015. Timing the origins of multicellular eukaryotes
1002 through phylogenomics and relaxed molecular clock analyses. Evolutionary transitions to
1003 multicellular life. Advances in Marine Genomics. Ruiz-Trillo I, Nedelcu AM (Eds.).
1004 Netherlands: Springer. P. 3–29.
- 1005 Signorovitch AY, Buss LW, Dellaporta SL. 2007. Comparative genomics of large mitochondria
1006 in Placozoans. *PLoS Genet* **3**:e13. doi:10.1371/journal.pgen.0030013
- 1007 Simion P, Philippe H, Baurain D, Jager M, Richter DJ, Di Franco A, Roure B, Satoh N,
1008 Quéinnec É, Ereskovsky A, Lapébie P, Corre E, Delsuc F, King N, Wörheide G, Manuel
1009 M. 2017. A large and consistent phylogenomic dataset supports sponges as the sister group
1010 to all other animals. *Curr Biol* **27**:958–967. doi:10.1016/j.cub.2017.02.031

- 1011 Smirnov AV. 2000. Subclass Aconchulina. In: Alimov AF, editor. Protista. Pt. 1. Handbook on
1012 zoology. St-Petersburg. Nauka. pp. 485–490.
- 1013 Srivastava M, Begovic E, Chapman J, Putnam NH, Hellsten U, Kawashima T, Kuo A, Mitros T,
1014 Salamov A, Carpenter ML, Signorovitch AY, Moreno MA, Kamm K, Grimwood J,
1015 Schmutz J, Shapiro H, Grigoriev IV, Buss LW, Schierwater B, Dellaporta SL, Rokhsar
1016 DS. 2008. The *Trichoplax* genome and the nature of placozoans. *Nature* **454**: 955–960. doi:
1017 10.1038/nature07191
- 1018 Srivastava M, Simakov O, Chapman J, Fahey B, Gauthier ME, Mitros T, Richards GS, Conaco
1019 C, Dacre M, Hellsten U, Larroux C, Putnam NH, Stanke M, Adamska M, Darling A,
1020 Degnan SM, Oakley TH, Plachetzki DC, Zhai Y, Adamski M, Calcino A, Cummins SF,
1021 Goodstein DM, Harris C, Jackson DJ, Leys SP, Shu S, Woodcroft BJ, Vervoort M, Kosik
1022 KS, Manning G, Degnan BM, Rokhsar DS. 2010. The *Amphimedon queenslandica* genome
1023 and the evolution of animal complexity. *Nature* **466**: 720–726. doi: 10.1038/nature09201
- 1024 Suga H, Ruiz-Trillo I. 2013. Development of ichthyosporeans sheds light on the origin of
1025 metazoan multicellularity. *Dev Biol* **377**:284–292. doi:10.1016/j.ydbio.2013.01.009
- 1026 Suga H, Chen Z, de Mendoza A, Sebé-Pedrós A, Brown MW, Kramer E, Carr M, Kerner P,
1027 Vervoort M, Sánchez-Pons N, Torruella G, Derelle R, Manning G, Lang BF, Russ C, Haas
1028 BJ, Roger AJ, Nusbaum C, Ruiz-Trillo I. 2013. The *Capsaspora* genome reveals a
1029 complex unicellular prehistory of animals. *Nat Commun* **4**:2325. doi:10.1038/ncomms3325
- 1030 Tikhonenkov DV, Mazei YA, Embulaeva EA. 2008. Degradational Succession of a
1031 Community of Heterotrophic Flagellates in Microcosm Experiments. *Zh Obshch*
1032 *Biol* **69**:57–64
- 1033 Tikhonenkov DV, Janouškovec J, Mylnikov AP, Mikhailov KV, Simdyanov TG, Aleoshin VV,
1034 Keeling PJ. 2014. Description of *Colponema vietnamica* sp.n. and *Acavomonas peruviana*
1035 n. gen. n. sp., two new alveolate phyla (Colponemidia nom. nov. and Acavomonidia nom.
1036 nov.) and their contributions to reconstructing the ancestral state of alveolates and
1037 eukaryotes. *PLoS ONE* **9**:e95467. doi:10.1371/journal.pone.0095467
- 1038 Torruella G, Derelle R, Paps J, Lang BF, Roger AJ, Shalchian-Tabrizi K, Ruiz-Trillo I. 2012.
1039 Phylogenetic relationships within the Opisthokonta based on phylogenomic analyses of
1040 conserved single-copy protein domains. *Mol Biol Evol* **29**:531–544.
1041 doi:10.1093/molbev/msr185
- 1042 Torruella G, de Mendoza A, Grau-Bové X, Antó M, Chaplin MA, del Campo J, Eme L, Pérez-
1043 Córdón G, Whipps CM, Nichols KM, Paley R, Roger AJ, Sitjà-Bobadilla A, Donachie S,
1044 Ruiz-Trillo I. 2015. Phylogenomics reveals convergent evolution of lifestyles in close
1045 relatives of animals and fungi. *Curr Biol* **25**:2404–2410. doi:10.1016/j.cub.2015.07.053

- 1046 Whelan NV, Kocot KM, Moroz LL, Halanych KM. 2015. Error, signal, and the placement of
1047 *Ctenophora* sister to all other animals. *Proc Natl Acad Sci USA* **112**:5773–5778.
1048 doi:10.1073/pnas.1503453112
- 1049 Wickstead B, Gull K. 2012. Evolutionary biology of dyneins. In: King S, editor. *Dyneins*.
1050 Elsevier. pp. 89–121.
- 1051 Williams F, Tew HA, Paul CE, Adams JC. 2014. The predicted secretomes of *Monosiga*
1052 *brevicollis* and *Capsaspora owczarzaki*, close unicellular relatives of metazoans, reveal
1053 new insights into the evolution of the metazoan extracellular matrix. *Matrix Biol* **37**:60–68.
1054 doi:10.1016/j.matbio.2014.02.002
- 1055 Yubuki N, Leander BS. 2013. Evolution of microtubule organizing centers across the tree of
1056 eukaryotes. *Plant J* **75**:230–244. doi:10.1111/tpj.12145
- 1057 Zakhvatkin AA. 1949. The comparative embryology of the low invertebrates. Sources and
1058 method of the origin of metazoan development. Moscow, Soviet Science. p. 395. (in
1059 Russian).
- 1060 **Legends for videos**
- 1061 Video 1. Swimming of *Syssomonas multiformis* cell with rotation.
- 1062 Video 2. Attached cell of *Syssomonas multiformis* and rapid flagellum beating.
- 1063 Video 3. Amoebflagellate stage of *Syssomonas multiformis*. Cells of eukaryotic prey
1064 *Parabodo caudatus* are also visible.
- 1065 Video 4. Loss of flagellum in *Syssomonas multiformis* and transition to amoeba.
- 1066 Video 5. Transformation of amoeba into a cyst in *Syssomonas multiformis*.
- 1067 Video 6. Palintomic divisions inside the cyst of *Syssomonas multiformis*.
- 1068 Video 7. Division into two cell structures in *Syssomonas multiformis*.
- 1069 Video 8. Cell and cyst of *Syssomonas multiformis* with vesicular structures inside.
- 1070 Video 9. Feeding of *Syssomonas multiformis* on eukaryotic prey.
- 1071 Video 10. Feeding of *Syssomonas multiformis* on bacteria.
- 1072 Video 11. Temporary cell aggregations of *Syssomonas multiformis*.
- 1073 Video 12. Floating rosette-like aggregation of *Syssomonas multiformis*.
- 1074 Video 13. Syncytium-like structures and budding of young flagellated daughter cells in
1075 *Syssomonas multiformis*.
- 1076 Video 14. Joint feeding of *Pigoraptor vietnamica* on died cell of *Parabodo caudatus*.
- 1077 Video 15. Joint feeding of *Pigoraptor chileana* on died cell of *Parabodo caudatus*.
- 1078 Video 16. Temporary cell aggregation of *Pigoraptor chileana*.
- 1079 **Videos are available at**
- 1080 **<https://drive.google.com/drive/folders/1ewNvwSQCAVG81eYjJPdhR41aBpUKR05L>**